

# REPORT DOCUMENTATION PAGE

Public reporting burden for this collection of information is estimated to average 1 hour per response, including the time for reviewing instructions, searching existing data sources, gathering and maintaining the data needed, and completing and reviewing this collection of information. Send comments regarding this burden estimate or any other aspect of this collection of information, including suggestions for reducing this burden, to Washington Headquarters Services, Directorate for Information Operations and Reports (0704-0188), Washington, DC 20540-6001. Respondents should be aware that notwithstanding any other provision of law, no person shall be subject to a penalty for failing to comply with a collection of information if it does not have a valid OMB control number. PLEASE DO NOT RETURN YOUR FORM TO THE ABOVE ADDRESS.

AFRL-SR-AR-TR-04-

0017

1. REPORT DATE (DD-MM-YYYY)

12-11-2003

2. REPORT TYPE

Final

4. TITLE AND SUBTITLE

DIRECT FORMATION OF SILANE COUPLING AGENTS ON GLASS  
FOR IMPROVED COMPOSITE PERFORMANCE

PERIOD COVERED (From - To)

04/2000 - 04/2003

5a. CONTRACT NUMBER

5b. GRANT NUMBER

F49620-00-1-0282

5c. PROGRAM ELEMENT NUMBER

5d. PROJECT NUMBER

5e. TASK NUMBER

5f. WORK UNIT NUMBER

6. AUTHOR(S)

Dr. David Boyles

Dr. Jon Kellar

Dr. William Cross

7. PERFORMING ORGANIZATION NAME(S) AND ADDRESS(ES)

South Dakota School of Mines and  
Technology

501 E. St. Joseph St.

Rapid City, SD 57701-3901

8. PERFORMING ORGANIZATION REPORT  
NUMBER

9. SPONSORING / MONITORING AGENCY NAME(S) AND ADDRESS(ES)

Air Force Office of Scientific Research

Organic Matrix Composites Program

4015 Wilson Blvd. Room 713

Arlington, VA 22203-1954

10. SPONSOR/MONITOR'S ACRONYM(S)  
AFOSR/VL

11. SPONSOR/MONITOR'S REPORT  
NUMBER(S)

12. DISTRIBUTION / AVAILABILITY STATEMENT

Approve for Public Release: Distribution Unlimited

13. SUPPLEMENTARY NOTES

20040130 055

14. ABSTRACT

This research resulted in the formation of hydrolytically stable, grafted silane coupling layers on glass surfaces. This was accomplished by: 1) hydrogenation of glass substrates; 2) synthesis of aminoalkenes; and 3) reaction of aminoalkenes with the reduced surface *via* a hydrosilylation reaction which formed the coupling agent directly on the surface of the glass fiber for glass surfaces incorporated into epoxy systems. In addition, chlorination of the glass surface followed by reaction with haloalkenes through a Grignard reaction, formed an unsaturated coupling agent on the glass surface for incorporation into vinyl esters based polymer systems. The grafted silane monolayers were identified through infrared spectroscopy, contact angle goniometry and x-ray photoelectron spectroscopy. Hygrothermal testing was performed by measuring the flexural strength and modulus in 4-point bending before and after environmental exposure. Both short-term (24 and 48 hours in boiling water) and long-term (5 week cycle having temperature and humidity values similar to aircraft exposure) hygrothermal tests were performed. In general, the grafted glass surfaces and composites made from this material proved more resistant to environmental exposure than untreated glass surfaces and glass surfaces treated with conventional silanes.

15. SUBJECT TERMS

polymer matrix composites, silane coupling agents, hygrothermal testing

16. SECURITY CLASSIFICATION OF:

a. REPORT  
UU

b. ABSTRACT  
UU

c. THIS PAGE  
UU

17. LIMITATION  
OF ABSTRACT

18. NUMBER  
OF PAGES

19a. NAME OF RESPONSIBLE PERSON  
Dr. David Boyles

19b. TELEPHONE NUMBER (include area  
code)  
(605) 394-1276

**DIRECT FORMATION OF SILANE COUPLING AGENTS ON GLASS  
SURFACES FOR IMPROVED COMPOSITE PERFORMANCE**

**Grant Number:** F49620-00-1-0282

**Principal Investigator:** Dr. David A. Boyles

Department of Chemistry and Chemical Engineering

**Co-Principal Investigators:** Dr. Jon J. Kellar

Department of Materials and Metallurgical Engineering

**Dr. William M. Cross**

Materials Engineering and Science Program

**Institution:**

**South Dakota School of Mines and Technology**

**Department of Chemistry and Chemical Engineering**

**501 E. St. Joseph Street**

**Rapid City, SD 57701-3995**



## TABLE OF CONTENTS

<b>TABLE OF CONTENTS .....</b>	<b>iii</b>
<b>LIST OF FIGURES .....</b>	<b>v</b>
<b>LIST OF TABLES .....</b>	<b>vii</b>
<b>EXECUTIVE SUMMARY .....</b>	<b>1</b>
Glass Slide and ATR Surface Modification.....	1
Glass Bead Surface Modification and Composite Formulation and Testing .....	2
Continuous Fiber Surface Modification and Composite Formulation and Testing .....	3
Weathering Of Surface-Modified, Single Fibers and Continuous-Fiber Composite Materials .....	5
<b>INTRODUCTION.....</b>	<b>7</b>
<b>GLASS SLIDE AND ATR SURFACE MODIFICATION .....</b>	<b>8</b>
Initial Work .....	8
Grafting on SiO <sub>2</sub> Slides.....	10
FT-IR Examination of Grafted Slides.....	11
Contact Angle Goniometry .....	14
Direct Grafting: SiO <sub>2</sub> Single Crystals .....	15
X-Ray Photoelectron Spectroscopy .....	18
<b>GLASS BEAD SURFACE MODIFICATION AND COMPOSITE FORMULATION AND TESTING .....</b>	<b>23</b>
FT-IR Examination of Grafted Powders .....	24
Grafting on Glass Beads.....	26
FT-IR Examination of Grafted Powders .....	29
Hydrolytic Stability.....	34
FT-IR Examination of Grafted Material.....	34
SEM Examination of E-glass Beads .....	34
Composite Formation .....	38
Mechanical Testing .....	38
SEM Examination of Fracture Surfaces.....	41
Hydrolytic Testing of Composites .....	44



<b>CONTINUOUS FIBER SURFACE MODIFICATION AND COMPOSITE FORMULATION AND TESTING .....</b>	<b>46</b>
Model System Selection .....	47
Fiber Preparation.....	47
Non-Traditional Silane Treatment.....	48
Silane Treatment.....	48
FT-IR Characterization.....	49
Mould Design and Fabrication .....	54
Continuous Fiber Composite Specimen Fabrication.....	54
3-Point Bend Testing (Ambient Conditions) .....	56
3-Point Bend Testing (Hygrothermal Evaluation).....	59
Optimization of the Curing Schedule of Polymer .....	60
4-Point Bend Testing (Hygrothermal Evaluation).....	65
 <b>WEATHERING OF SURFACE-MODIFIED, SINGLE FIBERS AND CONTINUOUS-FIBER COMPOSITE MATERIALS .....</b>	 <b>69</b>
Single Fiber Weathering Tests.....	69
Long Term Weathering Tests.....	71
 <b>RECOMMENDATIONS FOR FUTURE RESEARCH.....</b>	 <b>75</b>

## LIST OF FIGURES

Figure 1.	ATR Spectrum of DDA adsorbed on SiO <sub>2</sub> plate. ....	9
Figure 2.	Initial IR spectrum of grafted hexadecene after gentle rubbing with a paper towel to remove platinum black. ....	13
Figure 3.	IR spectrum of grafted hexadecene after acetone rinsing. ....	13
Figure 4.	Schematic showing the evanescent wave sampling technique. ....	17
Figure 5.	IR spectra showing Grignard/Undecenyl (evanescent wave) and 11-bromoundecene (transmission). ....	17
Figure 6.	Water droplets on grafted SiO <sub>2</sub> single crystal. ....	18
Figure 7.	XPS spectra of Si2p region of fiber samples. ....	20
Figure 8.	XPS spectra of Si2p region of e-glass samples. ....	21
Figure 9.	XPS spectra of Si2p region of ATR elements. ....	22
Figure 10.	IR spectra of hexadecene grafted to E-glass beads. ....	25
Figure 11.	Synthetic strategies adopted. ....	27
Figure 12.	Grafting of undecenylamine at a silica surface. A) Synthesis of undecenyl phthalimide. B) Grafting of undecenyl phthalimide and phthalimide deprotection. ....	28
Figure 13.	Grafting of chlorovinylbenzene to a chlorinated silica surface. ....	28
Figure 14.	Comparison of phthalimide (top/black spectrum) with allyl phthalimide (bottom/red spectrum). ....	30
Figure 15.	Comparison of phthalimide (top/black spectrum) with undecenyl phthalimide (bottom/red spectrum). ....	30
Figure 16.	Comparison of allyl phthalimide (black spectrum) with grafted allylamine (red spectrum). ....	31
Figure 17.	Comparison of undecenyl phthalimide (top/red spectrum) with grafted undecenylamine (bottom/black spectrum). ....	31
Figure 18.	Comparison of chlorovinylbenzene (red spectrum) with grafted vinylbenzyl (black spectrum). ....	32
Figure 19.	Comparison of allylbromide (black spectrum) with grafted allyl (red spectrum). ....	33
Figure 20.	Comparison of undecenylbromide (black spectrum) with grafted undecenyl (red spectrum). ....	33
Figure 21.	Comparison of grafted vinylbenzyl before (top/black spectrum) and after (bottom/red spectrum) hydrolytic stability testing for 1 day in TFAA. ....	35
Figure 22.	Untreated E-glass bead, no TFAA exposure. ....	36
Figure 23.	Undecenylamine grafted E-glass, no TFAA exposure. ....	36
Figure 24.	APS treated E-glass bead after 1 day exposure to TFAA. ....	37

Figure 25.	Undecenylamine grafted E-glass bead after 1 day exposure to TFAA.....	37
Figure 26.	Typical tensile test specimens used for mechanical testing.....	39
Figure 27.	Typical stress-strain curves.....	40
Figure 28.	SEM micrograph of the fracture surface of epoxy filled with untreated E-glass beads.....	42
Figure 29.	SEM micrograph of the fracture surface of epoxy filled with APS treated E-glass beads.....	42
Figure 30.	SEM micrograph of the fracture surface of epoxy filled with undecenylamine grafted E-glass beads. ....	43
Figure 31.	SEM micrograph close-up of an E-glass bead on the fracture surface of epoxy filled with allylamine grafted E-glass beads. ....	43
Figure 32.	Comparison of as received silica fibers (top spectrum) with plasma treated fibers (bottom spectrum). ....	50
Figure 33.	Comparison of undecenyl treated silica fibers (top spectrum) with plasma treated fibers (bottom spectrum).....	51
Figure 34.	Comparison of APS treated silica fibers (top spectrum) with plasma treated fibers (bottom spectrum). ....	52
Figure 35.	Comparison of undecenyl treated silica fibers before (top spectrum) and after boiling (bottom spectrum).....	53
Figure 36.	Comparison of APS treated silica fibers before (top spectrum) and after boiling (bottom spectrum). ....	53
Figure 37.	Schematic of mould for fabricating continuous fiber composite samples.....	55
Figure 38.	Picture of actual mould used for fabrication of continuous fiber composite samples.....	55
Figure 39.	Mould with fibers laid up. ....	56
Figure 40.	Picture of samples after 3-point bend testing.....	57
Figure 41.	Optical image of SiO <sub>2</sub> fibers within Derakane matrix (x50). ....	57
Figure 42.	Optical image of SiO <sub>2</sub> fibers within Derakane matrix (x20). ....	58
Figure 43.	Change of flexural moduli of Derakane with time at elevated temperature (post cure at 100°C). ....	64
Figure 44.	Change of flexural strength of Derakane with time at elevated temperature (post cure at 100°C). ....	64
Figure 45.	Comparison of broken samples after 3-point bending test and 4-point bending.....	66
Figure 46.	Environmental cycle, representative of the temperature /humidity condition an aircraft may meet during actual use. RH stands for relative humidity. ....	73

## LIST OF TABLES

Table 1.	Contact Angle and Surface Coverage for Hexadecene Grafted Slides.....	15
Table 2.	Contact Angle of Water and Percent Coverage of Grafted Silane Coupling Agent on SiO <sub>2</sub> Crystal as a Function of Time in Boiling Water .....	18
Table 3.	Summary of FT-IR Hydrolytic Stability Data .....	35
Table 4.	Summary of Mechanical Testing Data.....	40
Table 5.	Young's Modulus of Composites After Hydrolytic Exposure .....	45
Table 6.	Tensile Strength of Composites After Hydrolytic Exposure.....	46
Table 7.	Summary of FT-IR Hydrolytic Stability Data .....	54
Table 8.	Typical Dimensions and Specifications of Bend Test Samples .....	56
Table 9.	3-Point Bend Testing Results (Ambient Conditions).....	59
Table 10.	Flexural Moduli of Composite Samples Before and After Exposure to Boiling Water for 24 Hours .....	61
Table 11.	Flexural Moduli of Composite Samples Before and After Exposure to Boiling Water for 48 Hours .....	62
Table 12.	Flexural Strength of Composite Samples Before and After Exposure to Boiling Water for 24 Hours .....	62
Table 13.	Flexural Strength of Composite Samples Before and After Exposure to Boiling Water for 48 Hours .....	63
Table 14.	Mechanical Property Data of Derakane with Time at Elevated Temperature (Post Cure at 100°C).....	65
Table 15.	4-Point Bend Testing Results (Ambient Conditions).....	67
Table 16.	Flexural Moduli of Composite Samples Before and After Exposure to Boiling Water for 48 Hours .....	68
Table 17.	Flexural Strength of Composite Samples Before and After Exposure to Boiling Water for 48 Hours .....	68
Table 18.	Characteristic Fiber Strength (Mean) and 95% Confidence Interval (95% CI) for Various Fiber Treatments .....	71
Table 19.	The Relative Humidity and Salt Solution Abridged from ASTM E-104.....	73
Table 20.	Average Flexural Modulus and Strength Before and After Long-Term Weathering.....	74



## **EXECUTIVE SUMMARY**

The objective of the research is the formation of a hydrolytically stable, grafted silane coupling layer on glass surfaces for the inclusion into polymers to afford improved composite materials with enhanced properties. To achieve this objective research was conducted in four primary areas. Initial work in which glass slides and silica attenuated total reflectance crystals were modified with grafted silane coupling agents. This initial work was followed by research in which glass beads were surface modified and dispersed into polymers to form polymer matrix composite materials (PMCs). These PMCs were then tested both mechanically and for hydrolytic stability. The third area of research was the modification of continuous glass fibers and the incorporation of these surface modified fibers in PMCs. The continuous fiber-reinforced PMCs were subjected to mechanical and hydrolytic stability testing. Finally, the surface modified continuous fibers and PMCs manufactured from these fibers were subjected to short and long term weathering experiments.

### **Glass Slide and ATR Surface Modification**

Initial research was performed on glass slides and quartz attenuated total reflectance (ATR) elements. In this work the Speier route (surface chlorination followed by hydridization then grafting) was used. Hexadecene was the first material grafted. Infrared (IR) spectroscopy of the grafted material on the ATR elements showed the presence of aliphatic  $\text{-CH}_2$  bands from the hexadecene hydrocarbon chain. The crystal geometry and refractive index were used with the band heights to estimate a surface coverage of 40-50%. The contact angle measured for this surface was 64 degrees. The

contact angle can also be used to estimate the surface coverage from the Cassie-Baxter equation and for the angle found the corresponding surface coverage was 40%, which agrees well with the ATR estimate.

11-bromoundecene was grafted to the surface using a Grignard-reaction approach in which the quartz surface was first chlorinated then grafting was performed. IR spectroscopy using the ATR crystal again showed the presence of the hydrocarbon chains and the surface coverage as estimated to be 80%. Contact angle goniometry showed a 71 degree contact angle initially; the contact angle decreased to 63 degrees after 24-hours of boiling and to 42 degrees after 48-hours of boiling. These contact angles correspond to surface coverages of 80%, 65% and 30%, respectively. Thus, the ATR and contact angle estimates are substantially in agreement and boiling reduced the coverage by 19% after 24 hours and 62.5% after 48 hours.

#### **Glass Bead Surface Modification and Composite Formulation and Testing**

In the second area of the work, E-glass beads (both 4 and 35 microns in diameter) were subject to grafting both through the Speier route, resulting in grafted alkylamines, and through the Grignard route, resulting in double-bond terminated grafted material. Diffuse reflectance IR (DRIFT) spectroscopy was used to study the grafting products. The DRIFT spectra showed the presence of the grafted material. Hydrolytic stability of the grafted material was followed by exposing the grafted E-glass beads to trifluoroacetic acid (TFAA) for one-day. Depending on the grafted material, TFAA exposure resulted in the loss of at most 50% of the original amount grafted (allyl and undecenyl Grignard

grafts and undecenylamine Speier grafts) to at minimum 20% of the original grafted material (allylamine). As a comparison, aminopropyltrimethoxy silane (APS) coated beads lost 50-65% of their initial surface coverage due to TFAA exposure.

Alkylamine grafted E-glass beads were then dispersed into an epoxy resin for composite material testing. Both untreated and APS treated beads were also used for composite manufacture and testing as a comparison for the grafted bead composites. Uniaxial tensile testing was performed on the composites and the Young's modulus and tensile strength (TS) used to compare the samples. Addition of E-glass beads increased the Young's modulus of all composites over the pure matrix. Little difference was observed between the modulus values for all the composites, although the allylamine grafted beads may have given a slightly lower modulus. The allylamine and undecenylamine grafted composites gave a lower TS than any other system probably due to incomplete curing of the matrix as the epoxy was still tacky after the curing cycle was complete. All composite types were also subjected to 8-hours in boiling water as a hydrolytic exposure. The undecenylamine grafted composites showed the best strength retention (~70%). The other composites all lost 45-50% of their original strength. Thus, the undecenyl grafted E-glass beads performed best in terms of hydrolytic stability validating the premise of this research.

### **Continuous Fiber Surface Modification and Composite Formulation and Testing**

In addition to the glass bead work, continuous fiber reinforced composites were also studied. Quartzel fibers (+99.99% SiO<sub>2</sub>, 14 µm diameter) were used as the continuous



reinforcement and Derakane Momentum 470-300, an epoxy-vinyl monomer, was chosen as the polymer matrix. The Quartzel fibers were grafted with 11-bromoundecene through the Grignard route after the fibers were cleaned through an oxygen plasma process and hydrated following the plasma cleaning. Also, the grafted fiber composites were compared to composites with three types of fibers; 1) plasma treated to remove the pre-applied sizing, 2) plasma treated then hydrated fibers and 3) plasma, hydrated and APS treated. For these samples, 3-point and 4-point bending was performed due to limitations on manufacturing brought about by the use of continuous fibers. After treatment, some of the fibers were ground and examined by DRIFT to determine whether grafting had occurred. DRIFT spectra showed the presence of the hydrocarbon chains of the grafted material. Hydrolytic testing of the ground material showed that both the grafted fibers and APS treated fibers retained about 50% of their original coating after 1-day in boiling water.

Initial flexural testing performed using 3-point bend testing mainly showed that the cure schedule for the Derakane needed to be optimized with a post-cure cycle. Experiments with the pure polymer indicated that 5-hours at 373 K was sufficient for this work. With the new cure schedule, 4-point bend testing was used, as this is often more sensitive to interfacial behavior than 3-point bend testing. The flexural testing showed that the use of continuous fibers increased the flexural modulus and strength. Little difference between the fiber surface treatments was observed in the modulus, but the flexural strength was highly dependent on surface treatment and the grafted surface gave a much higher strength than the APS fibers. Plasma treated fibers gave the greatest strength. After

boiling the composites in water for 48-hours, 4-point bend testing was again performed to investigate the hydrolytic stability. The boiling caused little change in the flexural modulus for all sample types. The flexural strength decreased for all sample types, and the Grignard grafted undecenyl treated fibers gave the greatest strength of all samples.

### **Weathering Of Surface-Modified, Single Fibers and Continuous-Fiber Composite**

#### **Materials**

Short term weathering of single fibers showed that the Grignard grafting method developed in this work was the only surface treatment studied that retained its original strength after 24 hours boiling. Plasma-cleaned and hydrated fibers and silane-treated fibers lost 20-45% of their original strength. Long-term weathering meant to simulate typical environmental conditions seen by airplanes gave essentially the same results as boiling the samples for 48 hours.

Therefore, this work has proved the proposed concept; that coupling agents can be directly grafted to glass and silica surfaces, and that these coupling agents yield composites having improved hydrolytic stability and more resistance to environmental exposure than composites utilizing fibers having conventional surface treatments.

The results presented in this report are primarily the work of three graduate students, Mr. Hao Du, Mr. Dehong He and Mr. Cory Struckman. Mr. Du completed his Masters of Science degree in 2002 with his thesis entitled "Hydrolytic Stability Study of Directly Grafted Coupling Agents for Polymer Matrix Composites", which is available from the

Deveraux Library at the South Dakota School of Mines and Technology. Mr. He completed his Masters of Science degree in 2003 with his thesis entitled "Weathering Influence on the Mechanical Properties of Composite Materials", which is available from the Deveraux Library at the South Dakota School of Mines and Technology. Mr. Struckman is still completing his Masters of Science degree requirements and upon completion this thesis will be available from the Deveraux Library..

Mr. Struckman worked on this project throughout its entirety; Mr. Du worked on this project from its inception until his graduation in May 2002; and Mr. He worked on this project from August 2001 through the finish of the project. Currently two papers based on this research project are in preparation. The first is titled "Spectroscopic Examination of Grafted Coupling Agents" to be submitted *Applied Spectroscopy*, and the second is "Effect Of Environmental Exposure on the Flexural Properties of Polymer Matrix Composites Reinforced With Fibers Having a Novel Grafted Surface Treatment" to be submitted to *Composites, Part A*.

## INTRODUCTION

Polymer matrix composites (PMCs) made with reinforcements having silane coupling agents have drawbacks including some hydrolytic instability due to the lability of the Si-O linkage. In this project a new methodology which moved away from traditional coupling agents to a newer strategy for coupling agent modification of glass was explored. This new strategy replaced the long-standing use of trialkoxysilane coupling agents and instead relies on the grafting of an alkene directly to glass substrates.

Initial research involved using an SiO<sub>2</sub> glass slide and evanescent wave infrared spectroscopy to evaluate the formation of grafted silane layers. This portion of the research also involved contact angle goniometry to help ascertain the presence of grafted layers.

The next stage of the research involved grafting glass microspheres. Included in this research was hydrolytic stability testing of both the modified microsphere as well as composite specimen filled with the grafted microspheres.

The final stage of the research involved single fiber testing and composites with continuous fibers fabricated by a hand lay-up method. Both single, grafted fibers as well as composites were evaluated for hydrolytic stability and mechanical properties.

In summary, significant indirect evidence was found to indicate that the original proposed grafting synthesis was indeed possible. In addition, it was shown that composites

reinforced with grafted fibers were found to be superior to those reinforced with APS treated fiber (traditional silane coupling agent) when the absolute values of strengths were compared.

## GLASS SLIDE AND ATR SURFACE MODIFICATION

### Initial Work

The formation of modified glass surfaces has been performed on both glass powders and on glass slides this period. Attenuated total reflectance (ATR) and diffuse reflectance techniques were used for Fourier transform infrared (FT-IR) analysis. These techniques were chosen as they have been shown to be ideal for analysis of adsorbed/grafted surfactants on plates and powders, respectively.

Initially, ATR spectra were collected of dodecylamine (DDA) adsorbed on SiO<sub>2</sub> plates (50 mm x 20 mm x 1 mm) purchased from Harrick Scientific. DDA was chosen for initial research as its adsorption behavior on SiO<sub>2</sub> is well documented, and its IR spectrum is representative to that which is expected after successful silane grafting. The DDA was dissolved in distilled water at various concentrations and the slides were placed in the solution (one hour) to allow for adsorption. These SiO<sub>2</sub> plates were then evaluated by FT-IR spectroscopy in the region 2800-3000 cm<sup>-1</sup>. Shown in **Figure 1** is a spectrum of adsorbed DDA (from a 1 x 10<sup>-3</sup> M solution) on the SiO<sub>2</sub> plate. The IR region 2800-3000 cm<sup>-1</sup> was selected for evaluation, because this is the region where strong asymmetric and symmetric -CH<sub>2</sub> bands occur and the SiO<sub>2</sub> plates are transparent within this region. The

bands between  $2800\text{--}3000\text{ cm}^{-1}$  have been utilized in the past by the research team to give indications of surfactant surface coverage and alkyl chain conformation. In addition to FT-IR analysis, the  $\text{SiO}_2$  slides were also placed in a contact angle goniometer to measure the contact angle between the plates (with adsorbed DDA) and a sessile water droplet. An average contact angle of 55 degrees was found. Both the IR spectrum shown in **Figure 1** and the contact angle are representative of those reported in the literature for DDA adsorbed on  $\text{SiO}_2$ . Next, the slides were placed in a low frequency plasma asher in an attempt to remove the adsorbed DDA. To verify that the asher had indeed removed the adsorbed DDA the plates were once again subjected to ATR/FT-IR and contact angle analysis. It was found that the plasma asher completely removed any trace of the adsorbed DDA (as judged by a disappearance of relevant IR absorbance bands) and a near zero degree contact angle.

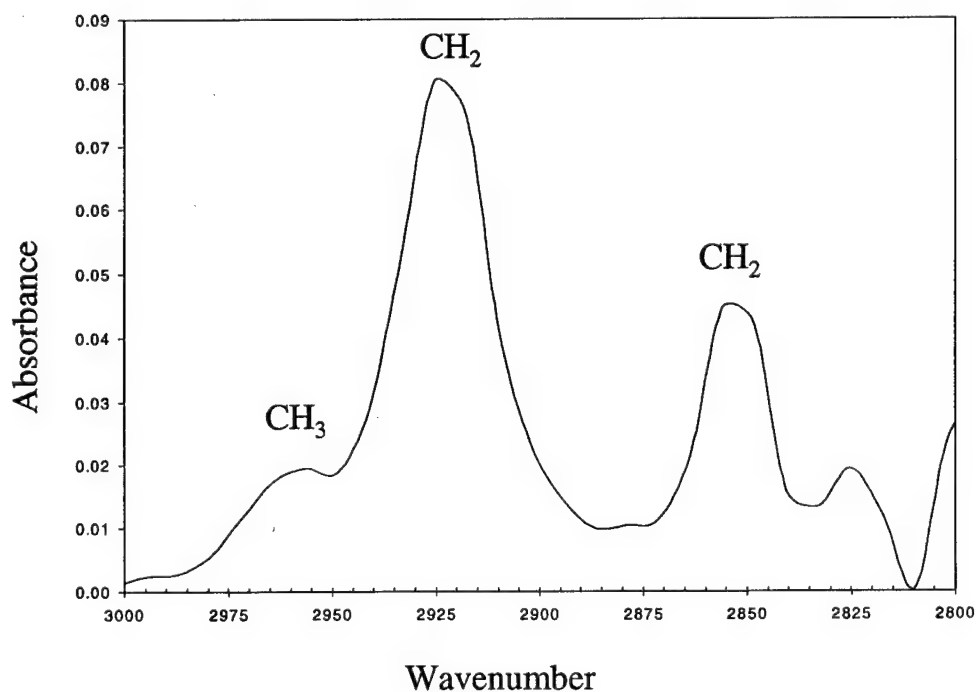


**Figure 1.** ATR Spectrum of DDA adsorbed on  $\text{SiO}_2$  plate.

### Grafting on SiO<sub>2</sub> Slides

The procedures for grafting to the glass slides are described below.

#### 1. Formation of Activated Si-Cl Glass Slide Surfaces

Thionyl chloride (15 mL) was added to dry toluene (50 mL) in a 100 mL round-bottomed flask. Two previously plasma-cleaned slides (Harrick Scientific Corp., 914-762-0020, Box 1288 / 88 Broadway Ossining, NY 10562, UV fused silica ATR crystal, 50 mm x 20 mm x 1 mm, 60 degree angle on face) were added and a water-cooled condenser with an argon inlet was affixed and the flask was purged with and kept under dry argon gas. The solution was heated at reflux for 96 hours. The flask was cooled to room temperature and the toluene solution was removed under argon using a canula. Owing to the sensitive nature of the Si-Cl bond and the extremely low surface area of the glass slides compared to the glass powders, the next step was conducted immediately without further manipulation of the slides.

#### 2. Formation of Activated Si-H Glass Slide Surfaces

Immediately after canulation of the toluene solution in the above step, 50 mL anhydrous ether was run into the flask over the glass slides via canula using dry argon as pressure gas. Lithium aluminum hydride (15 g) was added and the suspension was brought to reflux for 96 hours.

#### 3. Formation of Alkyl Grafted Glass Slide Surfaces

After completion of the previous step the lithium aluminum hydride/ether suspension was removed under dry argon pressure using a canula. The slides were rinsed twice with 50 mL portions of fresh, dry ether using canula technique under dry argon pressure. Dry

toluene (50 mL) was run into the flask and 15 mL of 1-hexadecene was added. Hydrochloroplatinic acid (0.01 g) was dissolved in 2-propanol (0.20 mL) and the resulting solution was added to the toluene solution, producing a pale yellow solution. The solution was refluxed 96 hours under argon. During the first 72 hours the solution remained yellow, but within the next 12 hours a scanty black precipitate of platinum which covered the inside wall of the flask and the slides was noted. The reflux was stopped after 96 hours; the slides were removed and were rinsed in air with several portions of ether, which did not effect removal of the black platinum precipitate.

#### **FT-IR Examination of Grafted Slides**

Following grafting of hexadecene to  $\text{SiO}_2$  slides, as described above, the grafted product was examined by both FT-IR spectroscopy and contact angle goniometry. For the FT-IR work, attenuated total reflectance (ATR) spectroscopy was used. In this technique, IR light is passed through a material such that attenuated total internal reflection occurs at the interface between the material and air. As the grafting was performed at this interface, the grafted hydrocarbon chain was sampled by the IR light yielding a spectrum of the grafted material similar to the adsorbed DDA spectrum in **Figure 1**.

**Figure 2** is a spectrum of the grafted layer obtained by the ATR technique following removal of the slide from the final grafting solution and after gentle rubbing with a paper towel. No IR light could be passed through the slide if the rubbing was not performed, owing to the presence of the gray film of finely divided platinum black on the slide surface. **Figure 2** clearly shows the presence of the grafted hexadecene, although the spectrum is of poor quality, making quantitation difficult. The grafted layer was



expected to resemble the spectrum of dodecylamine shown in **Figure 1**. In order to take every possible precaution against mixed results owing to chemisorption of organic rather than the desired chemical grafting, the slide was rinsed with acetone several times. As shown in **Figure 3**, acetone rinsing greatly improved the spectrum quality. The spectrum obtained was similar to the spectrum in **Figure 1**. Band heights in **Figure 3** were used to determine the amount of material grafted to the surface. In particular, the intense  $\text{CH}_2$  band centered at  $\sim 2925\text{ cm}^{-1}$  was used for two reasons. First, being the largest band in the spectrum, its use minimizes error due to noise. Second, if residual acetone were present in the grafted layer after rinsing, the  $\text{CH}_2$  band would not be affected since acetone--unlike hexadecene--contains no  $\text{CH}_2$  groups, which would affect the quantitation. To perform quantitative analysis, the length and thickness of the slide, the angle of incidence of the IR light at the slide-air interface and the absorptivity of the grafted layer were used as parameters. The absorptivity of the grafted layer was not measured, but the coverage was estimated using absorptivity data from other systems. This estimation indicated that the surface coverage is approximately 40-50% of a closely packed monolayer. The extent of this coverage depends upon the spacing of the silanol sites on the silica surface. Because the acetone used to remove excess hexadecene displays a  $-\text{CH}_2$  bending frequency at  $1431\text{ cm}^{-1}$  and a  $\text{C}=\text{O}$  stretching at  $1742\text{ cm}^{-1}$  the organic bands in the IR are clearly not due to acetone but to the grafted organic. Thus, the acetone rinse does in no way interfere with the  $\text{CH}_2$  band of hexadecene at  $2925\text{ cm}^{-1}$ . If the  $-\text{CH}_3$  band of acetone at  $2960\text{ cm}^{-1}$  had an affect on the hexadecene band such would have been apparent in the spectra.

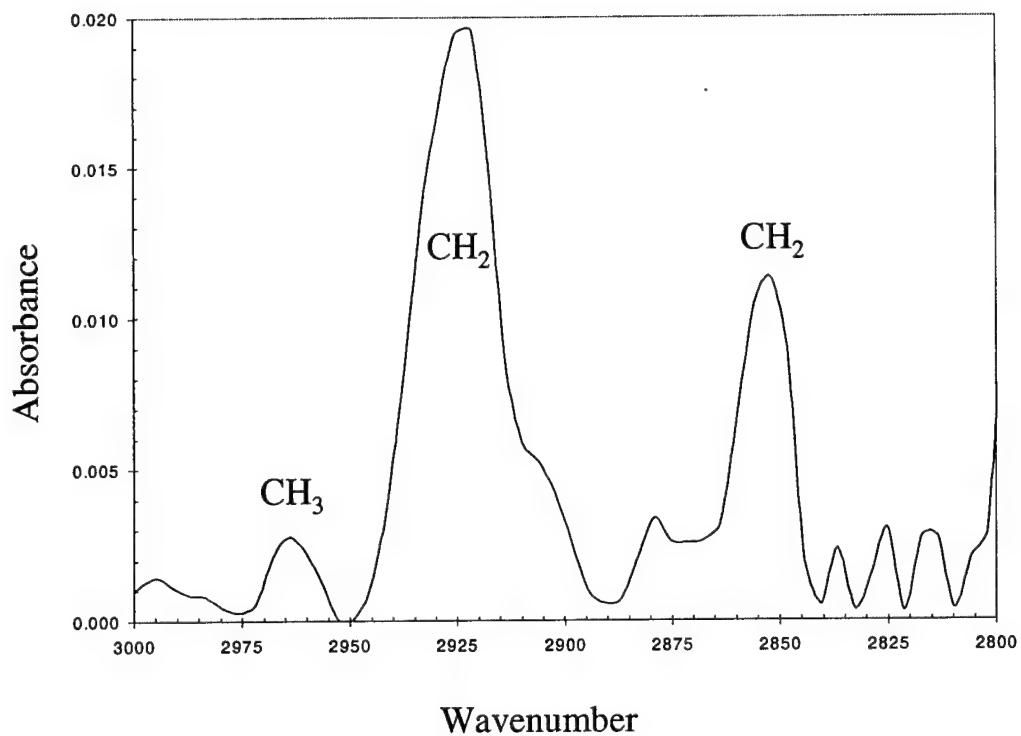


**Figure 2.** Initial IR spectrum of grafted hexadecene after gentle rubbing with a paper towel to remove platinum black.

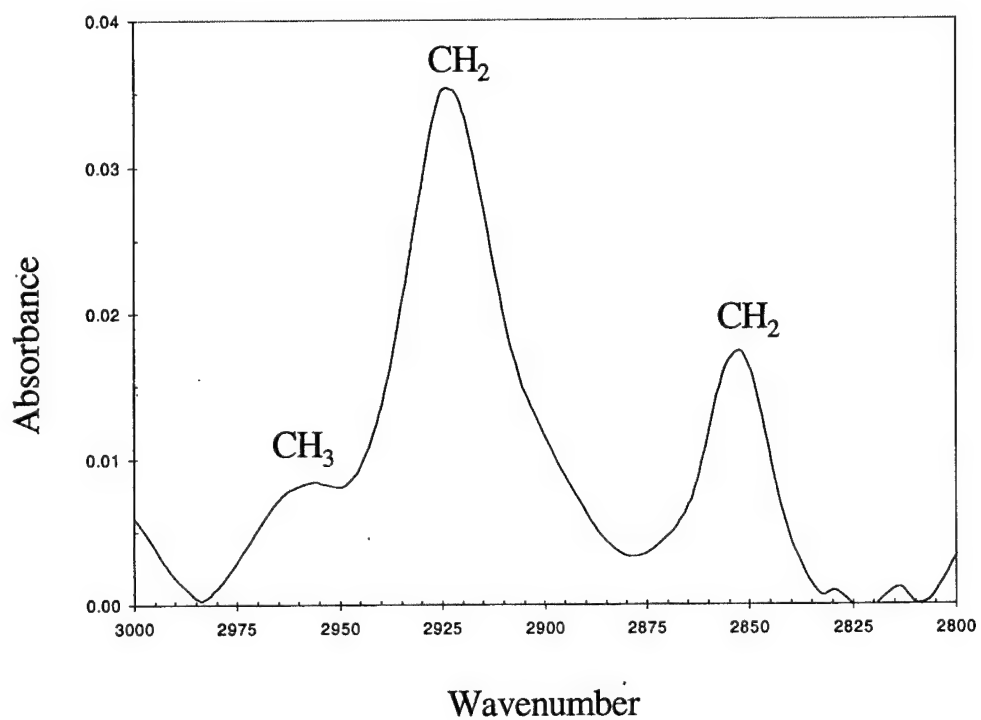


**Figure 3.** IR spectrum of grafted hexadecene after acetone rinsing.

### Contact Angle Goniometry

In addition to the FT-IR analysis, the slides were examined by contact angle goniometry to determine their hydrophobic character. In these experiments, similar to the dodecylamine treated slides, a sessile water droplet was placed on the surface and the three-phase contact angle was measured through the liquid phase. Cleaned, untreated slides exhibited a very small contact angle, usually between 0 and 5 degrees. Grafting of hexadecene to the slide surface was expected to significantly increase the contact angle, as treating silica surfaces with, for instance, octadecyltrichlorosilane, has been shown in the literature to yield a surface having contact angle between 110 and 115 degrees. **Table 1** summarizes contact angle measurements on several slides on which hexadecene was grafted using the procedure described previously. The average contact angles varied from 53.5 to 70.5 degrees with a grand mean of approximately 64 degrees. This indicates, once again, that the grafting procedure was successful. The contact angle value can also be used to estimate the surface coverage. The surface coverage can be estimated from the Cassie-Baxter equation:

$$\cos(\theta_c) = f_1 * \cos(\theta_1) + f_2 * \cos(\theta_2) \quad (1)$$

where  $f_1$  is the area fraction of grafted material with contact angle  $\theta_1$ ,  $f_2$  is the area fraction of ungrafted surface having a contact angle of  $\theta_2$  and  $\theta_c$  is the measured composite contact angle. Using the measured contact angles, and 113 and 0 degrees as  $\theta_1$  and  $\theta_2$ , respectively and realizing that  $f_1 + f_2 = 1$ , the surface coverage is estimated to be

40%, as shown in **Table 1**. This estimated surface coverage is thus in reasonable agreement with the value estimated from the ATR spectra.

**Table 1. Contact Angle and Surface Coverage for Hexadecene Grafted Slides**

Slide	Test Number	Mean Contact Angle ( $\theta$ )	Estimated Coverage (%)
1	1	53.5	29.1
2	1	70.5	47.9
2	2	64.2	40.6
2	3	64.8	41.3
2	4	66.1	42.8
Overall Mean		63.8	40.2

Using the measured contact angles, and 113 and 0 degrees as  $\theta_1$  and  $\theta_2$ , respectively and realizing that  $f_1 + f_2 = 1$ , the surface coverage is estimated to be 40%, as shown in **Table 1**. This estimated surface coverage is thus in reasonable agreement with the value estimated from the ATR spectra.

### **Direct Grafting: SiO<sub>2</sub> Single Crystals**

Direct grafting of silane coupling agent onto single crystals SiO<sub>2</sub> was also investigated. Single crystal SiO<sub>2</sub> was chosen as a model substrate as a mimic of Quartzel fibers that were used as reinforcements for the composite testing mentioned earlier. The same undecenyl surface treatment (e.g. Grignard reaction) was used with the single crystals of SiO<sub>2</sub>, as described earlier for the Quartzel fibers. The objective of use of SiO<sub>2</sub> single crystals in this manner was twofold, first to determine through evanescent wave infrared

(IR) spectroscopy evidence for successful grafting onto  $\text{SiO}_2$  substrates, and to use the grafted crystals for analysis of wetting. Shown in **Figure 4** is a schematic of the evanescent wave spectroscopic technique. One of the unique features of this method is its extreme surface sensitivity, ideal for analysis of direct grafting of silane coupling agents. Shown in **Figure 5** is a comparison between the evanescent wave IR spectrum of the  $\text{SiO}_2$  crystal after grafting and a transmission spectrum of 11-bromoundecene in the region  $3100\text{-}2800\text{ cm}^{-1}$ . Shown in both spectra are bands associated with the  $-\text{CH}$  stretching of the grafted layer and 11-bromoundecene. It can be seen that the two spectra are very similar, giving indirect evidence for the presence of the grafted silane coupling agent. In addition, however, IR spectroscopy cannot give direct evidence of Si-C bonding/grafting because of the opaque nature of the  $\text{SiO}_2$  crystal in the region of the IR where the Si-C band appears. Using the IR spectrum shown in **Figure 5** and method of Tillman et al. it was estimated that 80% of the  $\text{SiO}_2$  crystal was covered with grafted silane. Contact angle measurements (water) were also performed on the grafted  $\text{SiO}_2$  crystal as a function of time (24 and 48 hours) in boiling water. Water droplets are shown on the grafted crystal in **Figure 6** and the contact angle data as a function of time exposed to boiling water are presented in **Table 2**. From the change in surface coverage and contact angle it appears that some of the grafted silane is removed when subjected to boiling water.

## ATR IR Theory

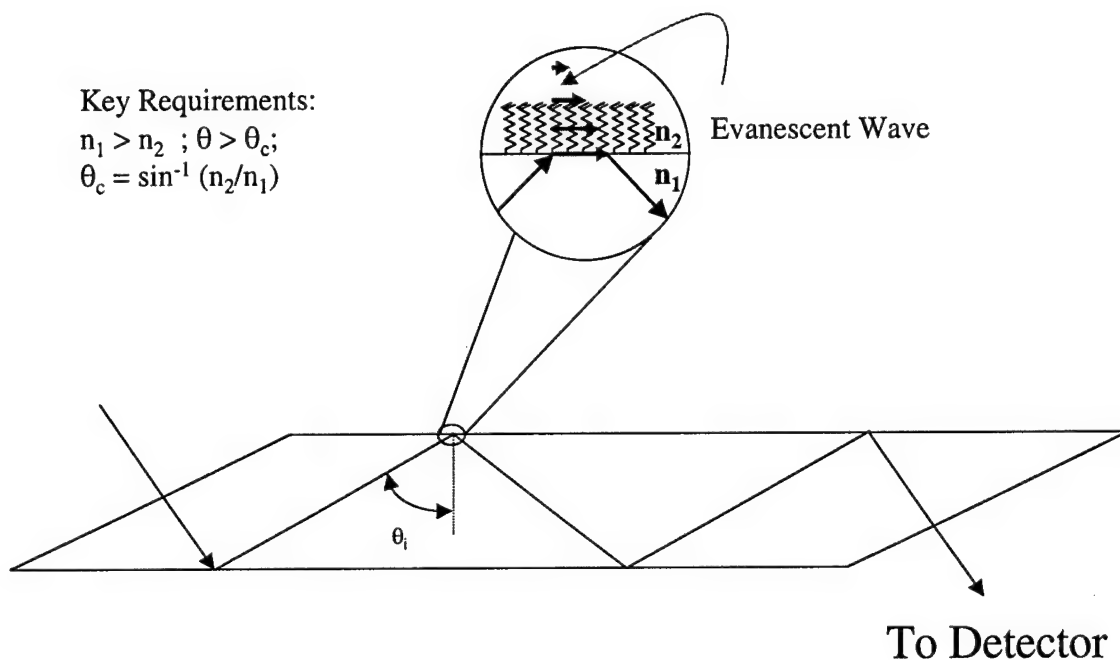


Figure 4. Schematic showing the evanescent wave sampling technique.

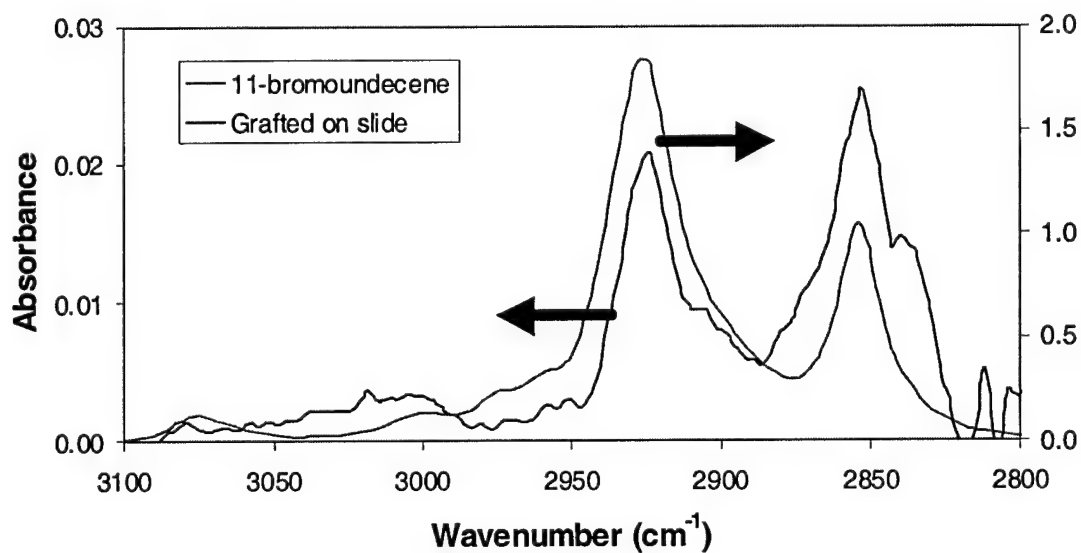
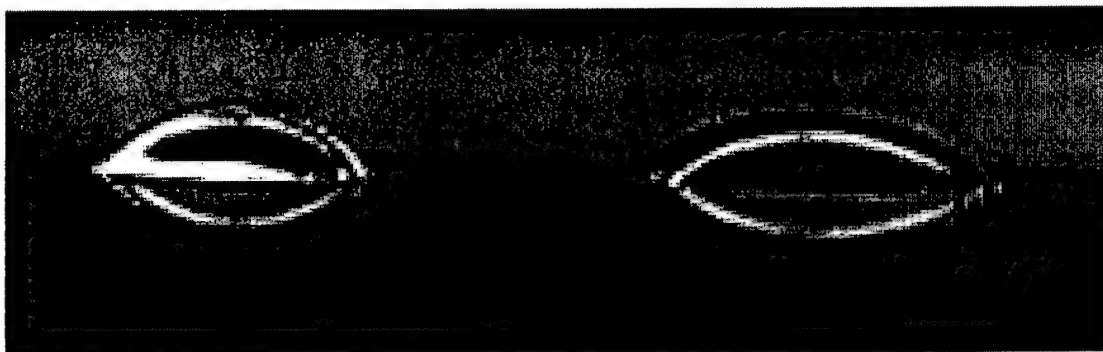


Figure 5. IR spectra showing Grignard/Undecenyl (evanescent wave) and 11-bromoundecene (transmission).



**Figure 6.** Water droplets on grafted SiO<sub>2</sub> single crystal.

**Table 2.** Contact Angle of Water and Percent Coverage of Grafted Silane Coupling Agent on SiO<sub>2</sub> Crystal as a Function of Time in Boiling Water

	Grafted	Grafted – 24 hour boil	Grafted – 48 hour boil
Contact Angle	70.9±7.0	62.5±5.5	41.9±7.5
% Coverage	~80	~65	~30

### **X-Ray Photoelectron Spectroscopy**

X-ray photoelectron spectroscopy (XPS) is a useful tool in determining the surface composition of a sample and the structure of the compounds present on that surface.

During XPS analysis, an X-ray beam causes electrons to be ejected from the surface of the sample being analyzed, and the kinetic energy of these electrons is measured.

Electrons from an atom with a higher positive charge in the nucleus require a larger kinetic energy for the electron to escape allowing for the determination of specific elements. A low-resolution scan can be used to show the elements present in a sample.

The bonds of a compound also affect the kinetic energy required to escape the sample so

compounds may be identified. After a low-resolution scan has determined which elements are present, a high resolution scan at the binding energy of the desired element can show the different bonds of the element. XPS is only effective through 3-4 atom layers because electrons from deeper in the sample cannot escape to the surface.

In an effort to identify the presence of Si-C bonds in grafted samples, XPS analysis was performed by our student researchers at the Environmental Molecular Sciences Laboratory at Pacific Northwest National Laboratory. The 3 sample substrate types examined were E-glass powders, SiO<sub>2</sub> fibers and fused silica slides.

The fibers were grafted with undecylamine prior to XPS examination. A wide scan of 3 separate samples of fibers was performed. The wide scan showed 26.06 atomic percent Si (Si2p peak ~102 eV) and 62.12 atomic percent O (O1s peak ~535 eV) bonds on the surface. Two regions of grafted fibers were tested; one was a discolored area of fiber from near the top of the reaction flask. This region showed a large amount of carbon on the surface, 82.60 atomic percent carbon, 13.7 % oxygen, and 5.43% silicon. The other region of grafted fibers was the area typically used to make composite samples. This area had 35.98 atomic percent carbon, 42.25% oxygen and 20.59 % silicon. As 3 to 4 layers of atoms is the extent of measurement, the coverage of carbon is slightly less than a monolayer. The Si2p region was examined in all 3 samples in an attempt to isolate a Si-C band, see **Figure 7**. Note the higher binding energies in the grafted and discolored sample. This may indicate the formation of Si-C bonds, but the data cannot be unambiguously interpreted.



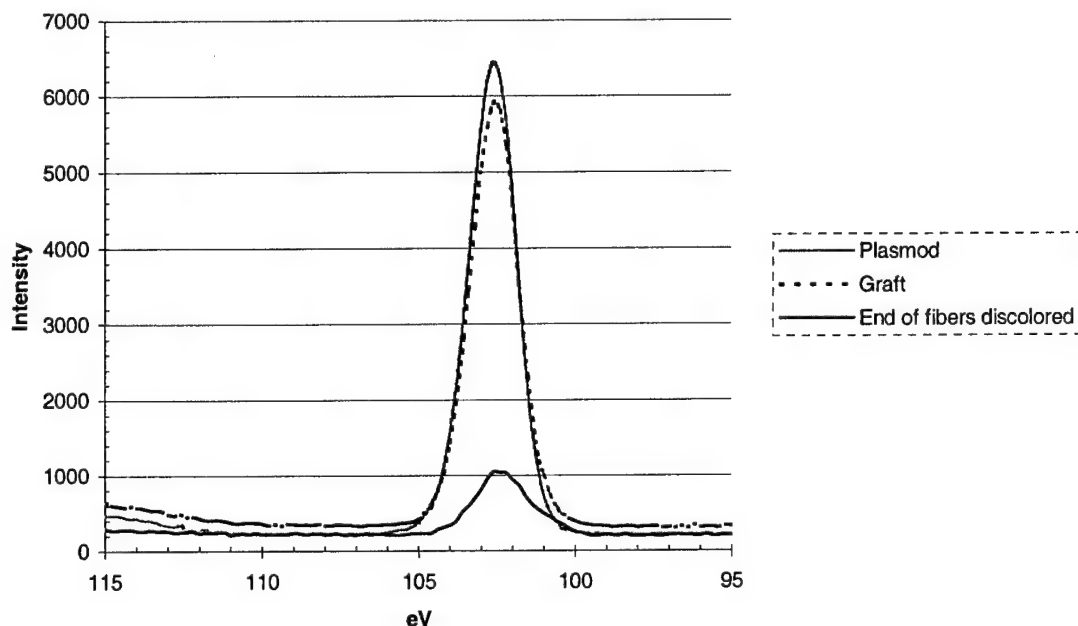


**Figure 7. XPS spectra of Si2p region of fiber samples.**

Four samples of E-glass beads were also examined. The first sample was a plasma treated sample as baseline. These particles had 14.16 atomic percent boron, 64.95% oxygen, 10.93 % silicon and 5.20% calcium. The second sample of particles tested was grafted with vinylbenzene using the Grignard route. This sample contained 91.49 atomic percent carbon and 8.51 % oxygen. As no silicon was present, the surface of the particles was completely covered with at least 4 layers of the grafted material. The third sample was the undecyl grafted E-Glass microspheres by the Grignard route. This sample showed 5.17 atomic percent carbon, 70.85% oxygen, 22.33% silicon and 1.65% calcium. The disappearance of the boron and reduction of the calcium indicated that the surface was changed by the reaction, which may have caused the low carbon content. The final sample of E-glass beads was grafted with an allyl group through the Grignard technique. This sample showed 5.38 atomic percent carbon, 71.53% oxygen, 20.93% silicon and 2.16% calcium. Similar to the undecenyl grafted surface, this sample had low

carbon and an absence of boron. The silicon Si2p peaks were compared in an effort to find Si-C binding energies, see **Figure 8**.

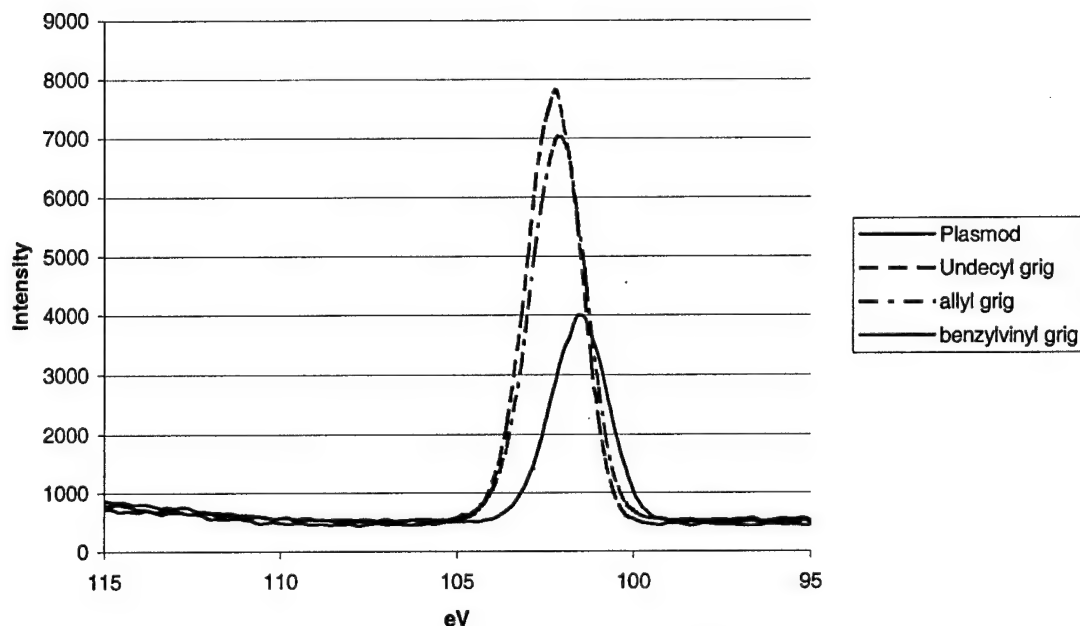


**Figure 8.** XPS spectra of Si2p region of E-glass samples.

Pure SiO<sub>2</sub> slides were the most recently prepared of all the samples. In an effort to preserve the grafted material the slides were not cleaned after the grafting process. The first slide was a plasma cleaned slide. This sample contained 15.83% carbon, 55.70% oxygen and 21.73% silicon as shown by a wide scan. Trace amounts of nitrogen, fluorine, aluminum, chlorine, potassium, calcium and zinc were also found on the sample. Many of these impurities are believed to be resultant from contamination of the oxygen used in the plasma. The second sample was the undecenyl grafted fibers. This sample exhibited 40.17% carbon, 42.79% oxygen, 12.15% magnesium, 3.58% silicon and 1.31% sulfur. The magnesium likely deposited on the surface during the grafting process as the Grignard route uses alkenylmagnesium halides. The atomic percents of the silicon and carbon indicated that slightly less than a monolayer of grafted material was

represent on the surface. The final slide was a grafted slide that had been boiled in water for 24 hours to simulate a weathering environment. This slide had 25.75 atomic percent carbon, 50.75% oxygen, 9.63% silicon, 5.49% nitrogen and 8.06% aluminum. The carbon atomic percent data indicate that about 35% of the carbon was removed from the surface, which is slightly more than the removal of material found by contact angle measurements, but similar to that shown by the IR spectra. The Si2p peaks of the slides were compared, see **Figure 9**. The slide samples were grounded in the spectrometer. All other samples were “floated” to attempt to remove shift in the Si2p peak. The peak shift remained present in the other samples. This may mean that a Si-C peak is present at 102.8 or that unequal charging is present in the samples containing more carbon.

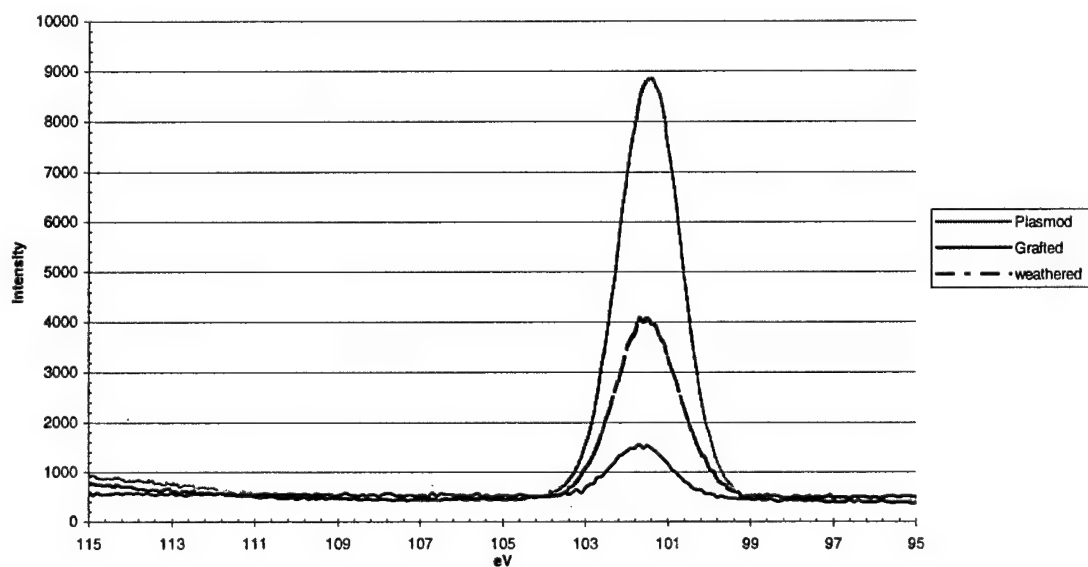


**Figure 9.** XPS spectra of Si2p region of ATR elements.

## GLASS BEAD SURFACE MODIFICATION AND COMPOSITE FORMULATION AND TESTING

Having demonstrated the effects of surface slide modification described previously, similar studies were undertaken on glass microspheres as they could be incorporated into resins to form polymer matrix composite materials. These studies served to provide information preparatory to continuous fiber composite formulation and testing.

Representative experimental procedures for the modification of the glass microspheres have been developed and follow below.

### 1. Formation of Activated Si-Cl Glass Powder Surfaces on Glass Microspheres

Thionyl chloride (15 mL) was added to dry toluene (50 mL) in a 100 mL round-bottomed flask. Glass powder (15 g) as Spherglass Solid Spheres 3000E (CAS 65997-17-3) from Potters Industrial, Inc., was added and a water-cooled condenser with an inlet was affixed to the flask which was purged with and kept under dry argon gas throughout the course of the reaction. The solution was heated at reflux for 96 hours. The flask was cooled to room temperature and the toluene solution was removed under argon using a canula. Residual solution was removed by two rinsings each of 30 mL anhydrous ether under dry argon using canula, allowing the suspension of glass powder to settle between rinsings.

### 2. Formation of Activated Si-H Glass Powder Surfaces

Anhydrous ether (50 mL) was run into the flask over the glass powder via canula using dry argon as pressure gas. Lithium aluminum hydride (15 g) was added and the suspension was maintained at reflux for 96 hours.

### 3. Formation of Alkyl Grafted Glass Powder Surfaces

After completion of the previous step the lithium aluminum hydride/ether suspension was removed under dry argon pressure using a canula. The glass powder was rinsed three times with 50 mL portions of fresh, dry ether using canula technique under dry argon pressure to remove residual lithium aluminum hydride, which has partial solubility in ether. Dry toluene (50 mL) was run into the flask and 15 mL of 1-hexadecene was added. Hydrochloroplatinic acid (0.01 g) was dissolved in 2-propanol (0.20 mL) and the resulting solution was added to the toluene solution, producing a pale yellow solution. The solution was refluxed 96 hours under argon. After cooling, the toluene solution was removed using canula and the glass powder was rinsed three times with 50 mL portions of ether. The product powder was light gray in color.

#### **FT-IR Examination of Grafted Powders**

Both 35 micron diameter and 4 micron diameter E-glass microspheres were utilized for grafting. The treated glass beads were characterized by Fourier transform infrared (FT-IR) spectroscopy using diffuse reflectance (DRIFT) spectroscopy. In this method the glass powders were admixed with nonabsorbing potassium bromide. The portion of the IR spectrum analyzed was the CH stretching region between 2800 and 3000  $\text{cm}^{-1}$ . The grafted hexadecene should contain 15  $\text{CH}_2$  moieties and 1  $\text{CH}_3$  moiety. The  $\text{CH}_2$  functional groups exhibit IR bands at  $\sim 2920$  and  $2850 \text{ cm}^{-1}$  while the primary  $\text{CH}_3$  stretching band occurs at  $\sim 2960 \text{ cm}^{-1}$ . The IR spectrum from each type of glass powder exhibits bands characteristic of the grafted hexadecene as shown in **Figure 3**. The bands of the grafted material on the 35 micron diameter microspheres were considerably more prominent than those on the 4 micron diameter beads, see **Figure 10**. As similar weights

of beads were placed in the diffuse reflectance accessory, the surface area of the 4 micron beads sampled was greater than the surface area of the 35 micron beads. Thus, the 35 micron beads were concluded to have more grafted material than do the 4 micron beads by a factor of at least 30. The precise surface coverages were not been measured but the surface coverage of the 35 micron E-glass beads was estimated to be less than 10%. The position of the asymmetric  $\text{-CH}_2$  stretching band ( $\sim 2920\text{ cm}^{-1}$ ) was used in the literature to measure the conformation and hence the aggregation of hydrocarbon molecules on surfaces. This band position typically varied from  $2915$  to  $2935\text{ cm}^{-1}$  depending upon the state of aggregation. The closer to  $2915\text{ cm}^{-1}$  the band position, the more aggregated are the hydrocarbon chains on the surface. The band position shown in **Figure 10** was  $2922\text{ cm}^{-1}$ . This indicates that the hydrocarbon chains are relatively tightly packed together, despite the rather low surface coverages.

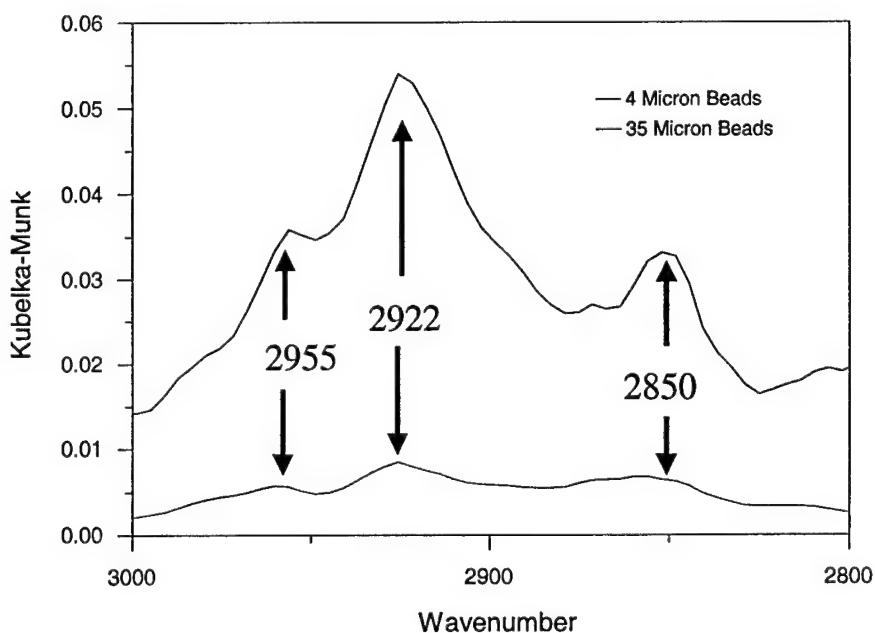


**Figure 10.** IR spectra of hexadecene grafted to E-glass beads.

The IR results indicated that the grafting procedure was successful on E-glass surfaces. These grafted beads prepared above were then used to manufacture composite tensile test specimens. Tensile testing was performed on the composite samples, and the Young's modulus and tensile strength were compared for epoxy filled with: 1. untreated E-glass bead, 2.  $\gamma$ -aminopropyltriethoxysilane (APS) coated E-glass bead, 3. allylamine grafted E-glass beads, and 4. undecylamine grafted E-glass beads. As the grafting process is expected to yield more hydrolytically stable surface coatings, the hydrolytic stability of the grafted material was also tested, first by etching the four treated bead types with aqueous trifluoroacetic acid (TFAA), then by examining the change in the IR spectrum of the adsorbed/grafted material. The E-glass beads with grafted material were shown to have enhanced resistance to the loss of surface grafted organic material from TFAA exposure than did the E-glass beads with the traditional APS treatment. In addition to etching the treated beads, the hydrolytic stability of the composite tensile test specimens prepared from the four treated bead types above was determined by tensile testing samples that had been boiled in water for 8 hours. The Young's modulus and tensile strength were compared for each treatment before and after environmental exposure, and the property change caused by environmental exposure was determined. Undecenylamine grafted E-glass filled composites exhibited the best overall resistance to hydrolytic exposure.

### **Grafting on Glass Beads**

Representative experimental procedures for the modification of the glass powders were developed. Two grafting strategies were followed, as depicted in **Figure 11**, the Speier

route and the Grignard Route. The Speier route was used to adapt the E-glass beads for compounding into epoxies. The Grignard route was also used and constituted an additional and more facile route affording modified E-glass to be reacted with monomers such as vinyl esters and others containing reactive double bonds. **Figure 12** shows the reaction sequence for synthesizing undecenylamine at a silica surface. A protocol similar to that given in **Figure 12a** was used to synthesize allyl phthalimide, graft this to a silica

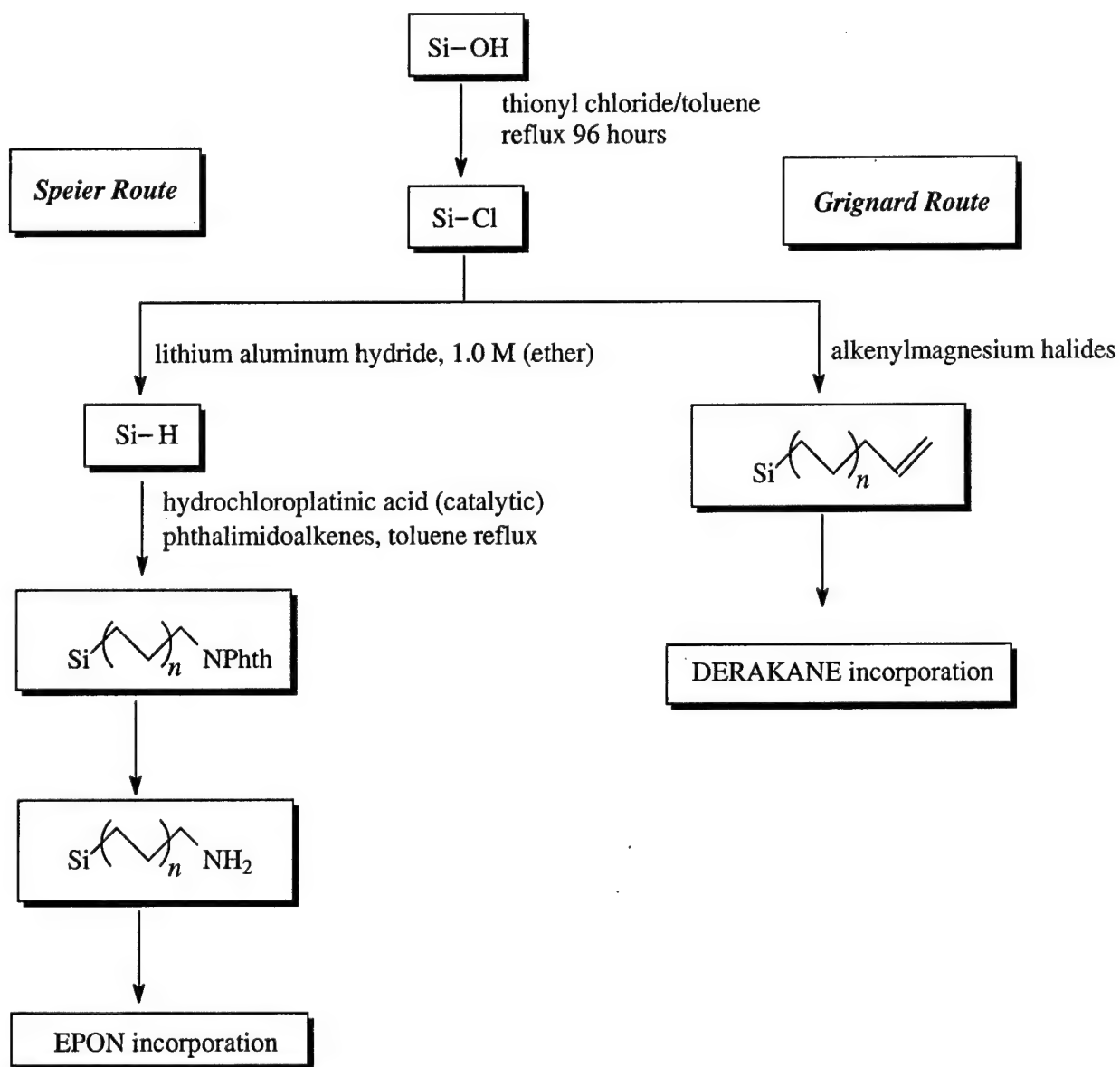


**Figure 11.** Synthetic strategies adopted.



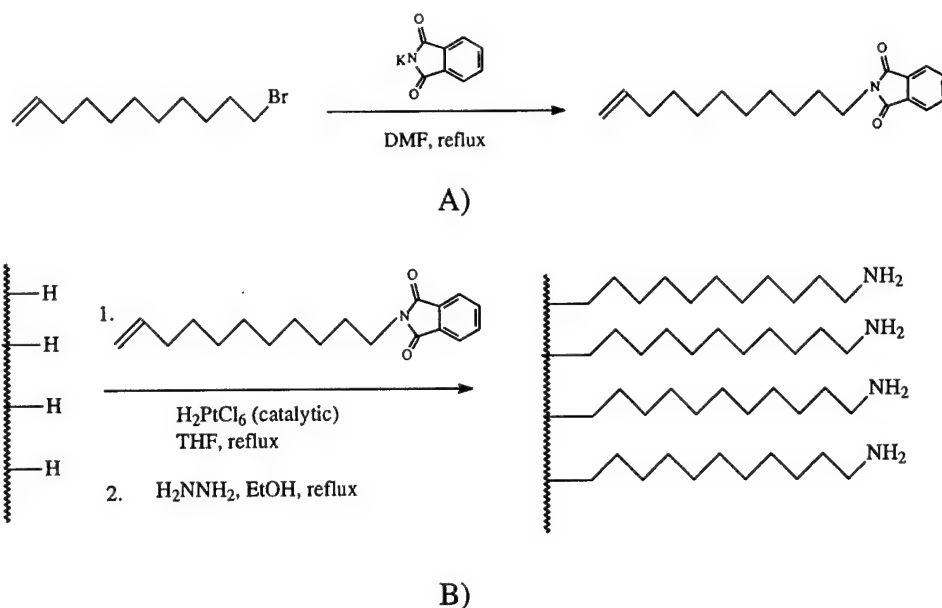


**Figure 12. Grafting of undecenylamine at a silica surface. A) Synthesis of undecenyl phthalimide. B) Grafting of undecenyl phthalimide and phthalimide deprotection.**

surface (following hydridization of the silica) and then deprotect the phthalimide group to a reactive amino group. see **Figure 12b**. **Figure 13** contains the Grignard route, which is useful for synthesis of surfaces for inclusion in vinyl polymer matrices. As **Figure 13** shows, this route was advantageous as the silica surface does not need to be hydridized after chlorination, and grafting can thus be accomplished in a single step. Allyl bromide and undecenyl bromide were grafted using procedures similar to that given in **Figure 12**.

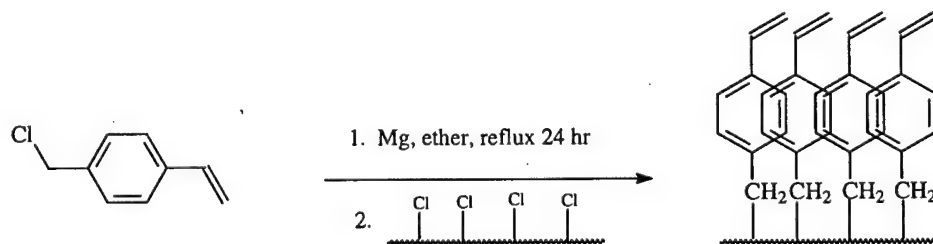


**Figure 13. Grafting of chlorovinylbenzene to a chlorinated silica surface.**

### **FT-IR Examination of Grafted Powders**

E-glass beads, 4 microns in diameter, utilized for grafting as previously described, were characterized by Fourier transform infrared (FT-IR) spectroscopy using diffuse reflectance (DRIFT) spectroscopy. For the phthalimides prior to grafting, the FT-IR spectra of the precursor phthalimides and the synthesized allyl- or undecenyl phthalimide were compared. **Figure 14** shows this comparison for allyl phthalimide, while **Figure 15** shows the comparison for undecenyl phthalimide. Examination of these two figures indicates that the products formed contain the desired phthalimide. Therefore, this material was grafted to hydridized E-glass surfaces and the phthalimide group was converted to an amino group so that the grafted E-glass surface would be compatible with epoxy resins. FT-IR spectroscopy was used to determine the success of the grafting and conversion reaction. **Figures 16 and 17** show a comparison of the allyl and undecenyl phthalimide CH stretching regions before grafting and the CH stretching region of the grafted material after conversion of phthalimide to amino groups. For both the allyl material (**Figure 14**) and the undecenyl material (**Figure 15**), the loss of the bands labeled  $\text{CH}_2=\text{CH}$  and aromatic CH indicated that grafting had occurred ( $\text{CH}_2=\text{CH}$ ) and that the phthalimide had been removed (aromatic CH). The retention of the bands labeled aliphatic CH indicated that the grafted material remained on the surface, as desired.

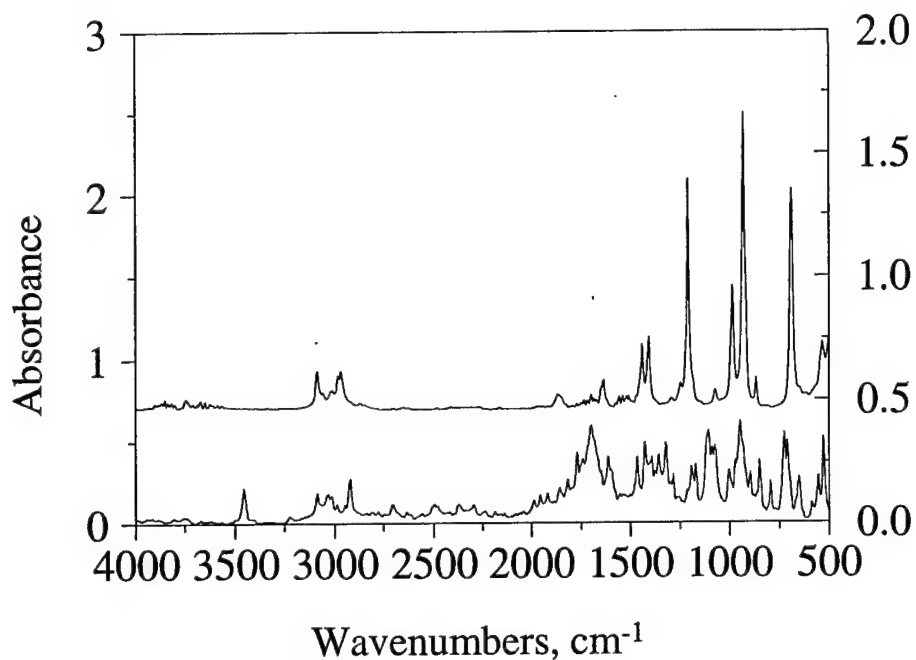


**Figure 14.** Comparison of phthalimide (top/black spectrum) with allyl phthalimide (bottom/red spectrum).

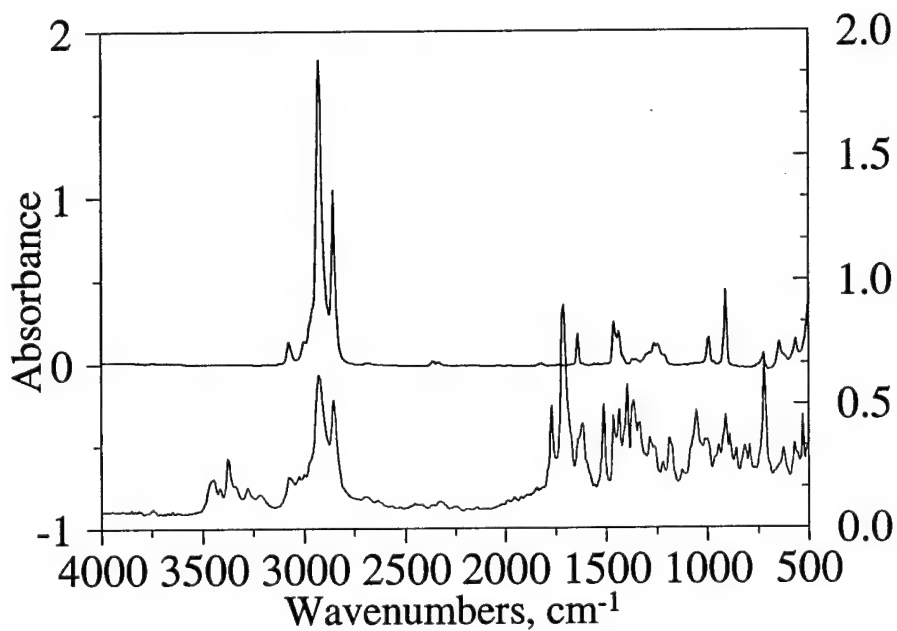


**Figure 15.** Comparison of phthalimide (top/black spectrum) with undecenyl phthalimide (bottom/red spectrum).

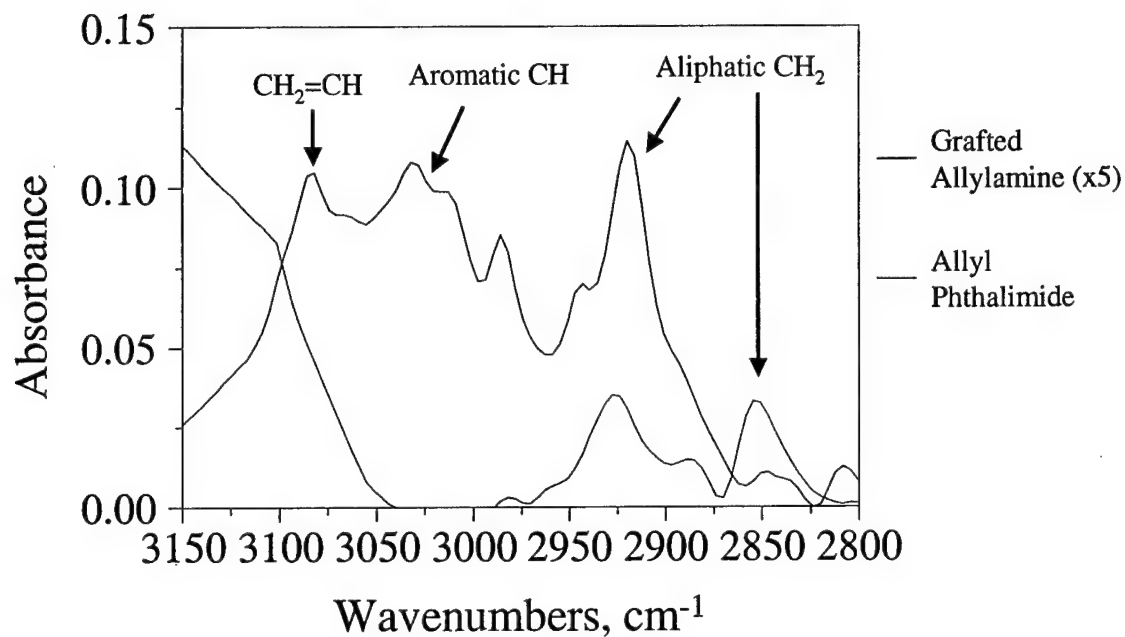


Figure 16. Comparison of allyl phthalimide (black spectrum) with grafted allylamine (red spectrum).

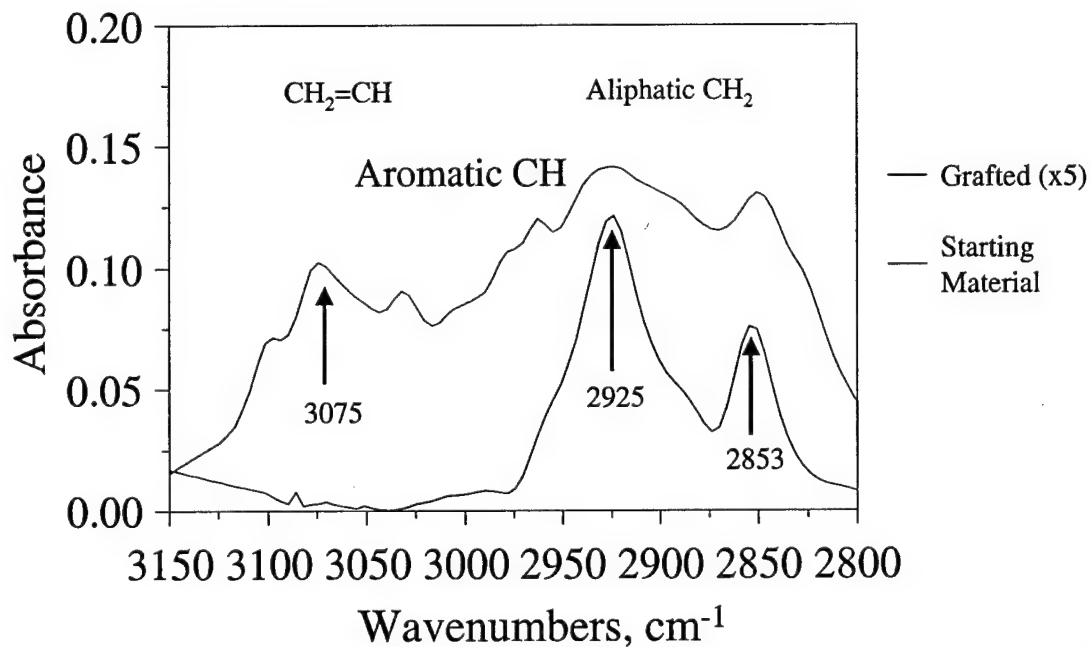
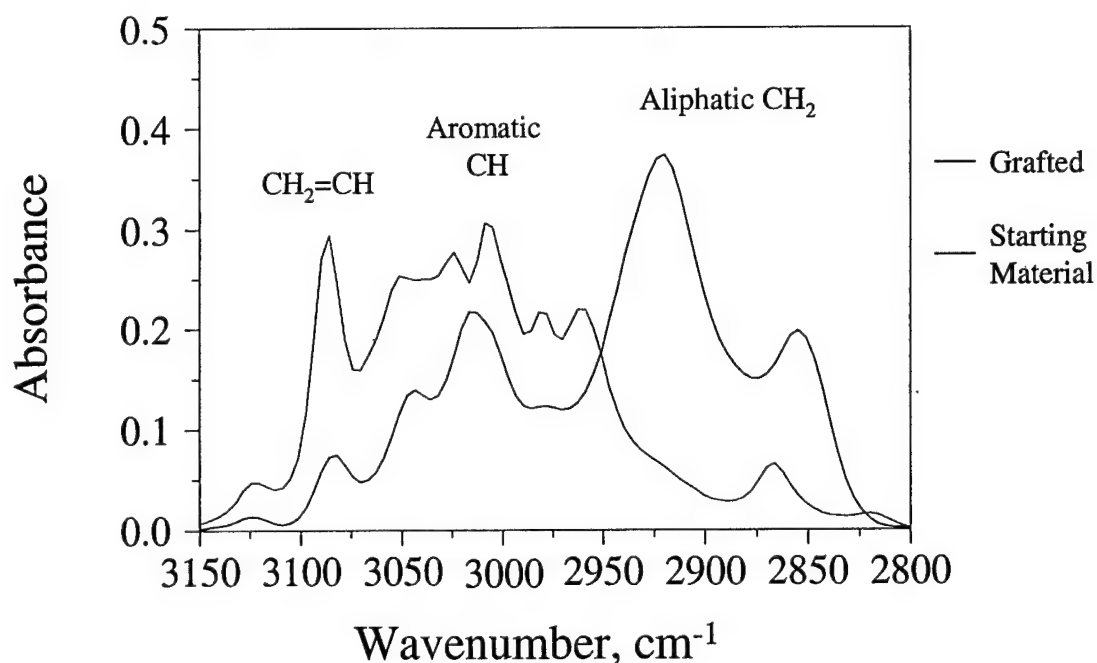


Figure 17. Comparison of undecenyl phthalimide (top/red spectrum) with grafted undecenylamine (bottom/black spectrum).

For the Grignard route, the FT-IR spectra of the initial components were compared with those of the grafted compounds to determine whether grafting had occurred. **Figure 18-17** show these spectra for vinylbenzyl Grignard grafting, allyl Grignard grafting and undecylenyl Grignard grafting. In **Figures 18-20**, grafting can be seen by the decrease in the band labeled  $\text{CH}_2=\text{CH}$ . This indicated that the Grignard reaction was successful. For the vinylbenzyl case (**Figure 18**), the  $\text{CH}_2=\text{CH}$  band did not decrease to zero because there appears to be some non-grafted material incorporated into the grafted layer. This may be explained by the strong interaction between the benzene rings, which resulted in adsorption of non-grafted material.



**Figure 18.** Comparison of chlorovinylbenzene (red spectrum) with grafted vinylbenzyl (black spectrum).

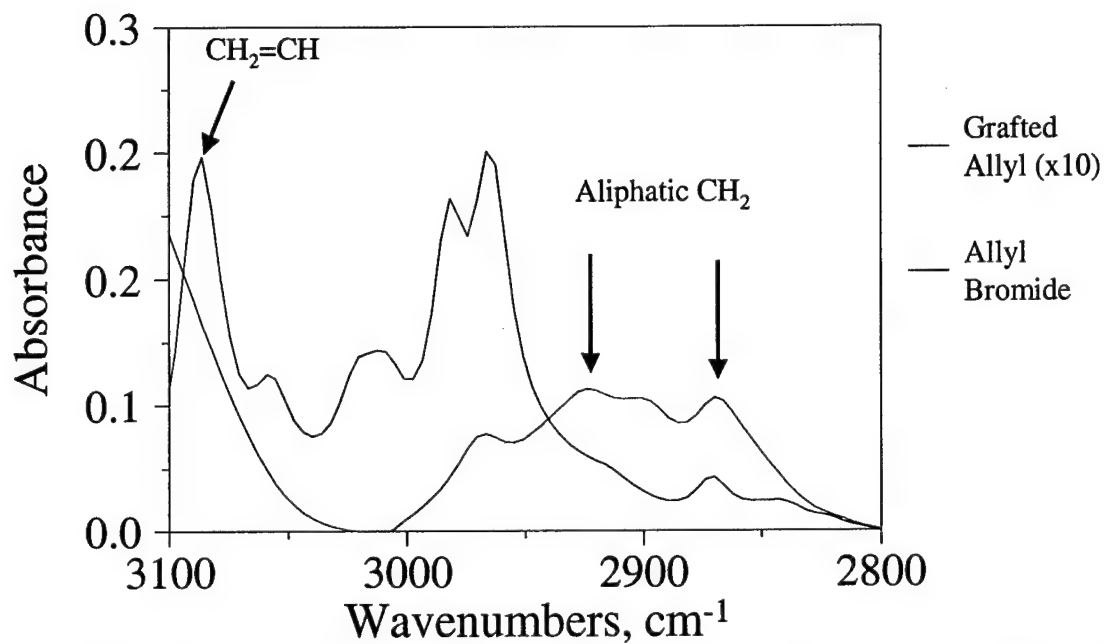


Figure 19. Comparison of allylbromide (black spectrum) with grafted allyl (red spectrum).

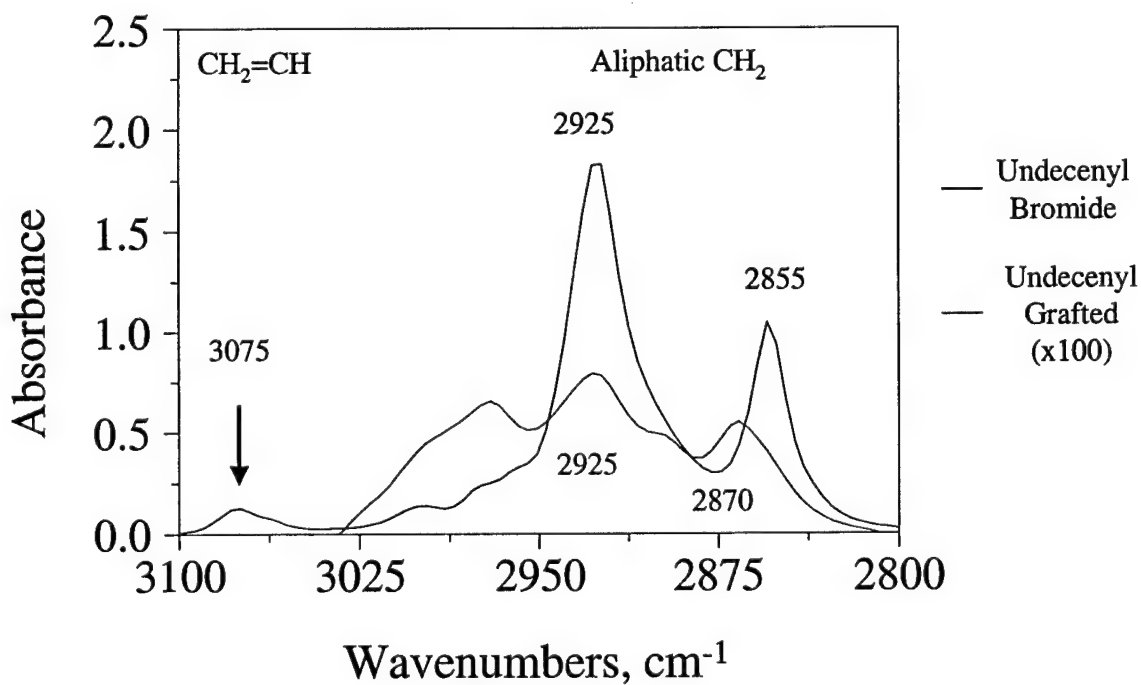


Figure 20. Comparison of undecenylbromide (black spectrum) with grafted undecenyl (red spectrum).

### **Hydrolytic Stability**

The hydrolytic stability of the grafted material on E-glass beads was tested by exposing the grafted beads to a 0.75 mmol solution of trifluoroacetic acid (TFAA) for 1 day. The FT-IR spectra of the grafted material were compared before and after exposure to TFAA. The amount of the grafted material remaining after 1 day in TFAA was determined and compared to the same beads with adsorbed APS that had been treated in the same manner. In addition, the surfaces of the E-glass beads were examined by scanning electron microscopy (SEM) to distinguish any morphological changes.

### **FT-IR Examination of Grafted Material**

**Figure 21** depicts a typical set of comparison spectra for grafted vinylbenzene (Grignard route) on E-glass beads. All the bands in the initial spectrum have decreased by approximately the same amount, as expected. **Table 3** contains a summary of the average amount of band height decrease for the grafted E-glass and for APS treated E-glass. **Table 3** shows that the grafted material was clearly superior to APS in terms of the amount of material removed from the surface by TFAA treatment. For instance, about 75-80% of grafted allylamine remained at the E-glass surface while only 35-50% of the APS remained adsorbed to the E-glass. Thus, grafting was approximately twice as successful at keeping material on the surface as adsorption from solution.

### **SEM Examination of E-glass Beads**

Following exposure to TFAA, some of the E-glass beads were examined by SEM. These samples were prepared by placing a small amount of beads on a glass slide

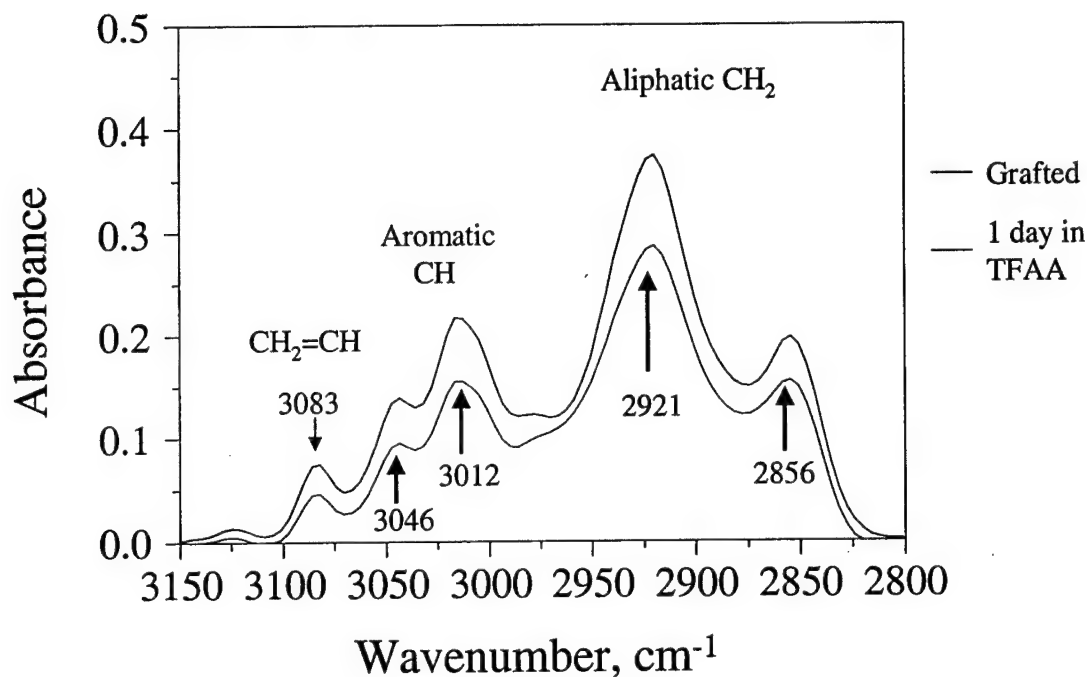


**Figure 21.** Comparison of grafted vinylbenzyl before (top/black spectrum) and after (bottom/red spectrum) hydrolytic stability testing for 1 day in TFAA.

**Table 3.** Summary of FT-IR Hydrolytic Stability Data

Material Tested	Percent remaining after 1 day in TFAA
Grafted Vinylbenzyl (Grignard route)	66-75
Grafted Undecenyl (Grignard route)	50-66
Grafted Undecenylamine (Speier route)	50-66
Grafted Allyl (Grignard route)	50-66
Grafted Allylamine (Speier route)	75-80
Adsorbed APS (1 wt% solution)	35-50

and dispersing the beads using acetone. These samples were carbon coated to allow individual particles to be observed. Micrographs of these individual particles were obtained and the E-glass bead surfaces were examined (**Figures 22-25**). Relatively few



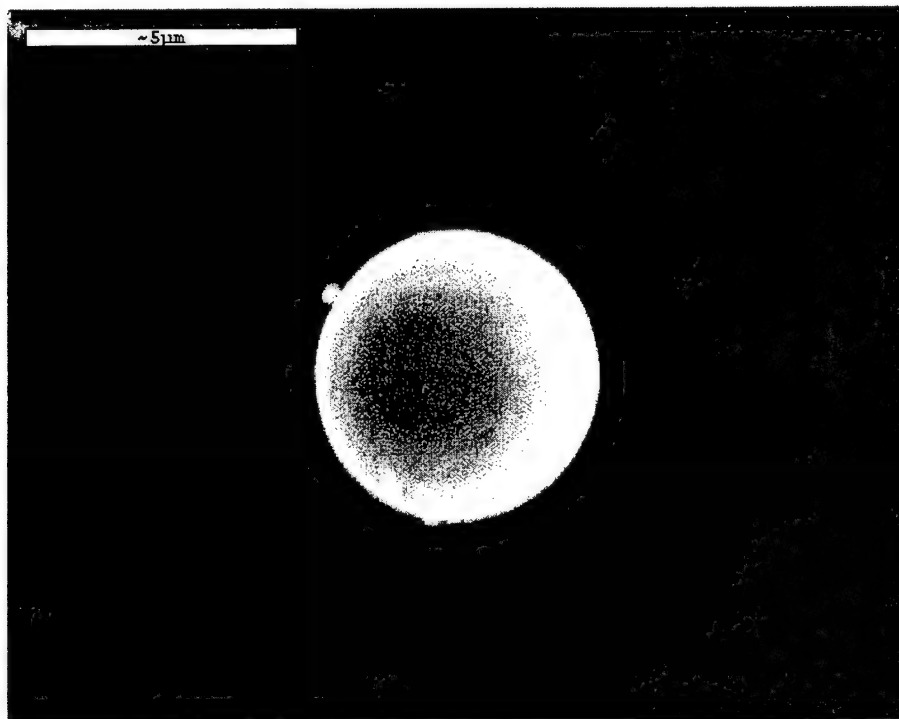


**Figure 22.**     **Untreated E-glass bead, no TFAA exposure.**

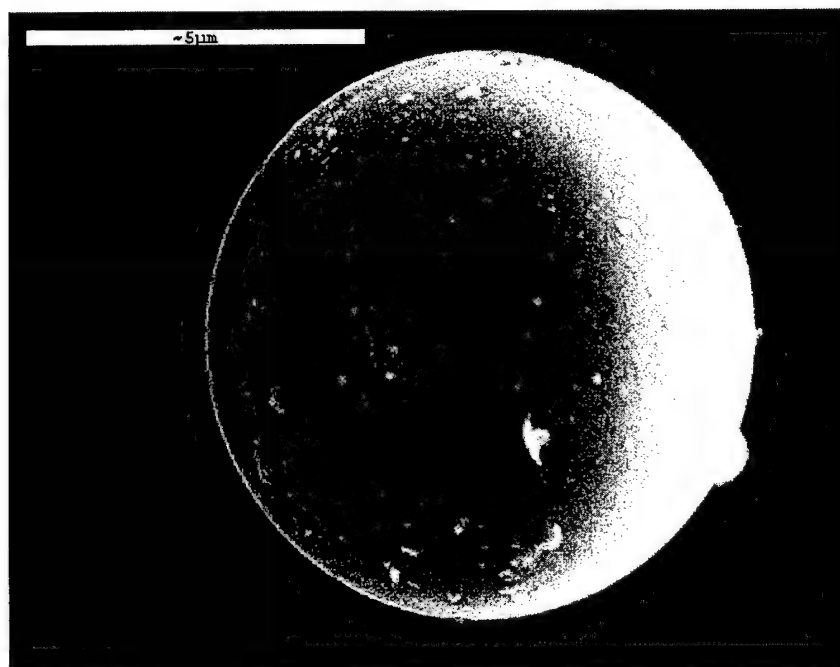


**Figure 23.**     **Undecenylamine grafted E-glass, no TFAA exposure.**

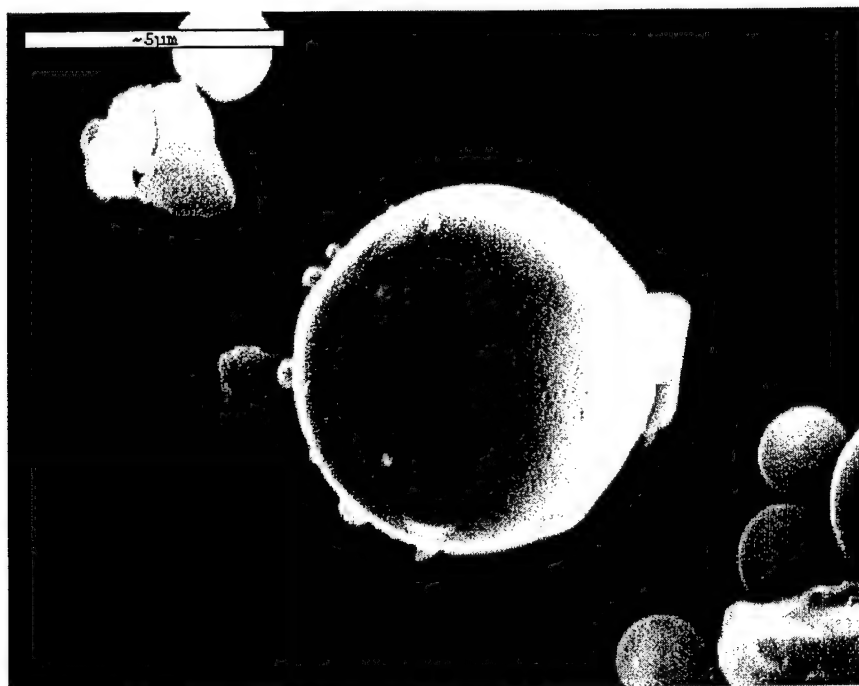


**Figure 24.** APS treated E-glass bead after 1 day exposure to TFAA.



**Figure 25.** Undecenylamine grafted E-glass bead after 1 day exposure to TFAA.

differences were observed between particles having various surface treatments. Surface striations were observed after TFSA treatment on all surfaces, which may be due to etching of the surface, by TFSA.

### **Composite Formation**

Following grafting to E-glass beads, composite materials were fabricated. Only epoxy matrix systems were used in this portion of the research. The epoxy resin used was Epon 828 (Resins-Versatics) cured with 27 phr methylene dianiline (MDA) curing agent. When utilized, E-glass beads (50% by weight) were compounded with the epoxy. Curing was accomplished by heating the mixture to 80 °C for 2 hours followed by heating at 150 °C for an additional 2 hours. Curing was performed in a vacuum oven operating at about 0.3-0.4 atmospheres. Five tensile test specimens were made of each sample type, and these samples were then used for tensile testing. **Figure 26** shows typical tensile test specimens used for mechanical testing. All 5 tensile test specimens were made at the same time from the same compounding.

### **Mechanical Testing**

**Figure 27** shows typical stress-strain curves for the various composites made and for pure epoxy cured in the same manner as the composites. From **Figure 27**, addition of E-glass beads increases the Young's modulus (initial slope of the stress-strain curve), while decreasing the tensile (maximum) strength. **Table 4** shows these trends more clearly.

Specifically, the Young's modulus has increased by about a factor of 2 from about 1.7

GPa to about 3.5 GPa. The different surface treatments do not exhibit much difference in Young's modulus. Although the grafted material composites do exhibit statistically different Young's moduli compared to the APS treated composite, none of the treated composites can be differentiated from the composite fabricated with untreated E-glass beads. For the tensile strength, little difference is seen between the pure epoxy, the untreated E-glass beads in epoxy and the APS treated E-glass beads in epoxy. The grafted E-glass beads exhibited slightly lower tensile strengths, which is probably related to the observation that, after curing, the tensile test specimens were still tacky. Thus, curing

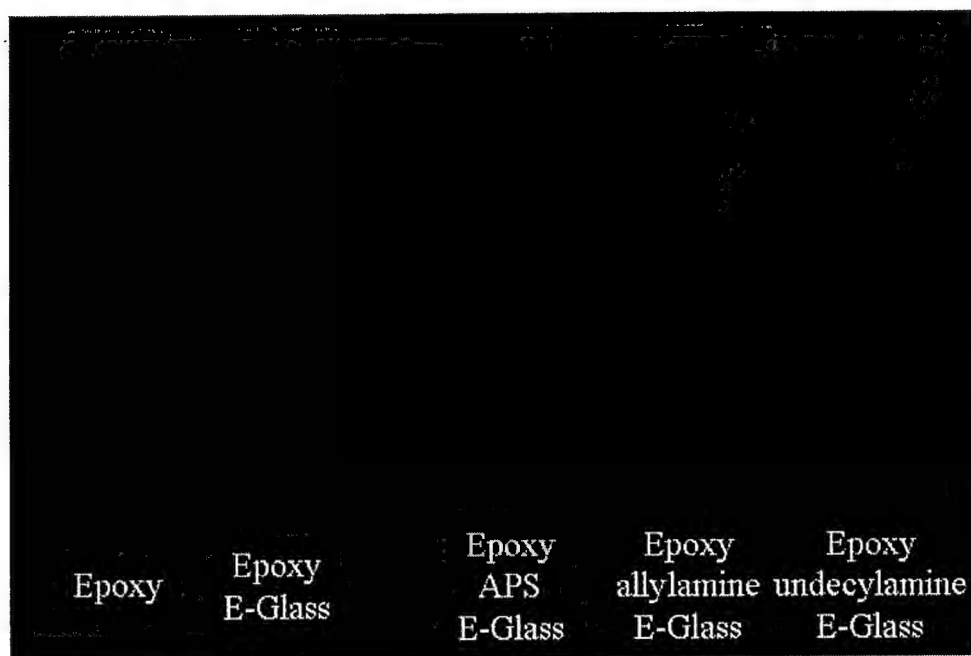


**Figure 26.** Typical tensile test specimens used for mechanical testing.

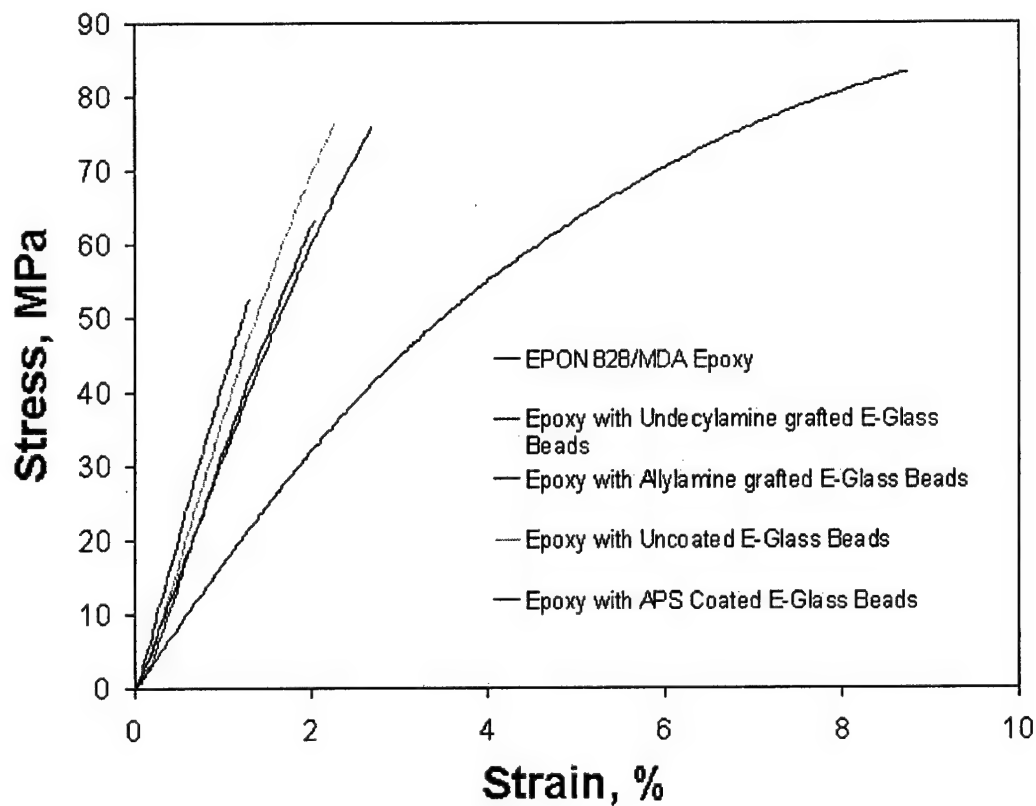


Figure 27. Typical stress-strain curves.

Table 4. Summary of Mechanical Testing Data

Material	Young's Modulus (GPa)	Tensile Strength (MPa)
Epon 828 with MDA	$1.68 \pm 0.07$	$81.5 \pm 3.0$
Epoxy with undecenylamine grafted E-Glass beads	$3.70 \pm 0.40$	$54.3 \pm 20$
Epoxy with allylamine grafted E-Glass beads	$3.61 \pm 0.27$	$62.6 \pm 1.6$
Epoxy with untreated E-Glass beads	$3.44 \pm 0.39$	$73.7 \pm 5.3$
Epoxy with APS treated E-Glass beads	$3.16 \pm 0.13$	$80.5 \pm 7.5$

was not completed for the grafted material in the same time that curing was completed for the pure epoxy and the non-grafting treatments. This indicates that the curing cycle was not optimized for the grafted E-glass bead composites leading to a decrease in mechanical properties.

### **SEM Examination of Fracture Surfaces**

After the composites were mechanically tested, the fracture surfaces were examined by SEM imaging. The primary purpose of this imaging was to assess the degree of wetting of the E-glass beads and to examine the dispersion of the E-glass beads in the composite. **Figure 28** shows an SEM micrograph of the fracture surface for a composite made with untreated E-glass beads. Several examples of beads pulled from the fracture surface are evident. In addition, the beads/microspheres do not seem to be wetted by the polymer. **Figures 29 and 30** show similar SEM micrographs for APS treated and undecenylamine grafted E-glass beads. Specifically, in both of these figures, the beads are well wetted by the polymer and few cavitations are observed. Thus, both APS treatment and undecenylamine grafting alter the surface chemistry of the E-glass beads to facilitate wetting, and both APS and the grafted material appear to allow adhesion to the polymer system. **Figure 31** shows a higher magnification view of an allylamine grafted E-glass bead indicating the wetting of the bead by the epoxy.

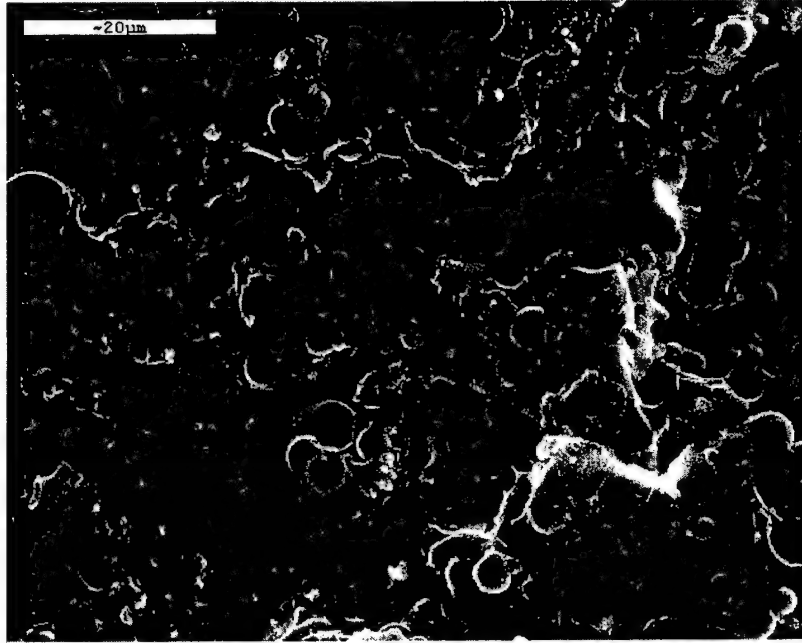


**Figure 28.** SEM micrograph of the fracture surface of epoxy filled with untreated E-glass beads.

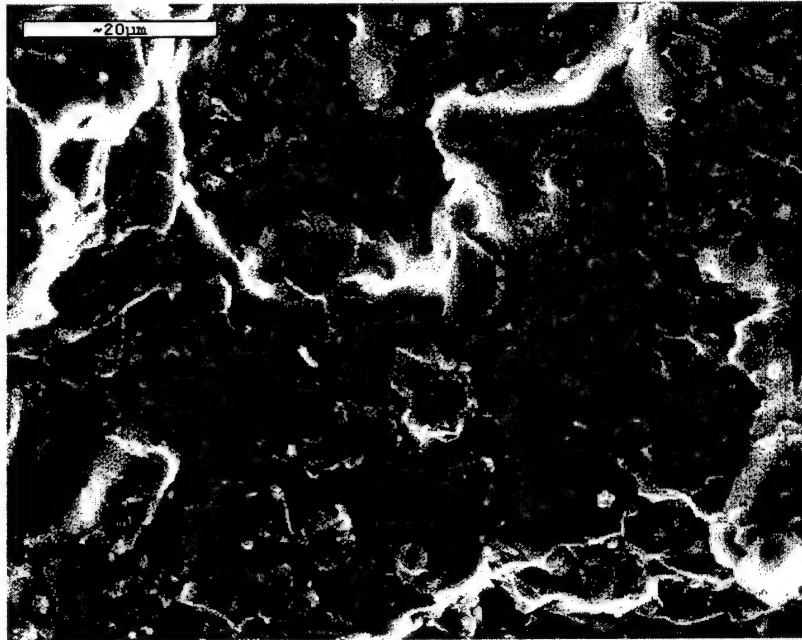


**Figure 29.** SEM micrograph of the fracture surface of epoxy filled with APS treated E-glass beads.

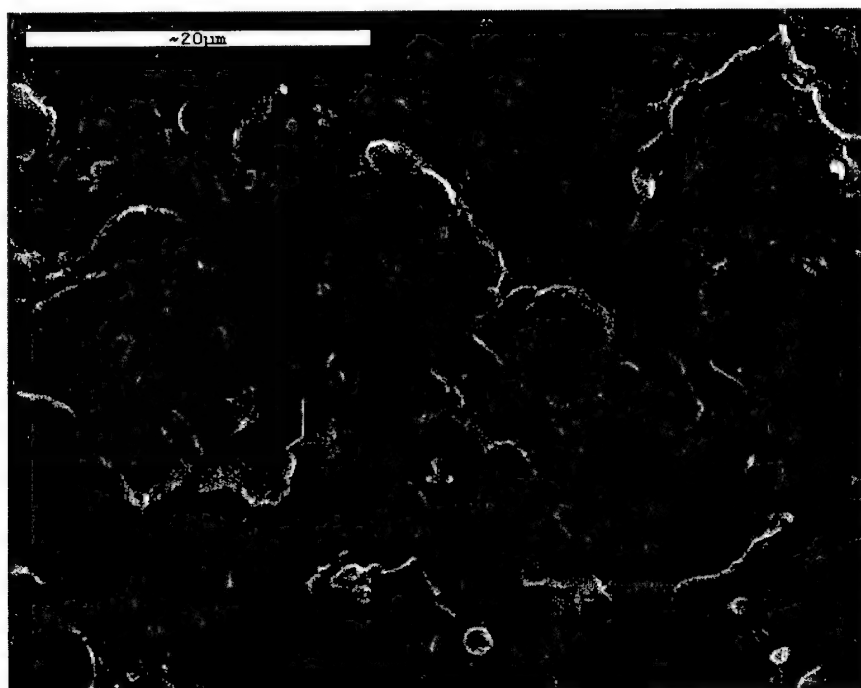


**Figure 30.** SEM micrograph of the fracture surface of epoxy filled with undecenylamine grafted E-glass beads.



**Figure 31.** SEM micrograph close-up of an E-glass bead on the fracture surface of epoxy filled with allylamine grafted E-glass beads.



### **Hydrolytic Testing of Composites**

After successful compounding of epoxy matrix composite materials, these composites were tested to determine their resistance to hydrolytic stability of the composite materials. Hydrolytic stability testing was performed by boiling tensile test specimens, similar to those shown in **Figure 19**, for 8 hours in water. The size and weight change of the samples were measured but were found to be less than 1% gain for all samples tested. Thus, the material does not incorporate much water during this exposure. Following hydrolytic exposure, the samples were subject to tensile testing. As before, the Young's modulus and the tensile strength were determined from the stress-strain curves. **Table 5** shows the results for Young's modulus obtained from tensile testing of hydrolytically exposed samples, while **Table 6** shows the resulting tensile strengths. With respect to the Young's modulus (see **Table 5**), all treatments displayed significant loss of stiffness. The undecenylamine grafted E-glass and the adsorbed APS treated E-glass filled composites exhibited the least loss of stiffness and the change from the non-hydrolytically treated composite was about the same in both cases. The loss in stiffness is not attributable to changes in the matrix as the pure matrix properties exhibited essentially the same Young's modulus whether or not it had been hydrolytically exposed. The tensile strength data exhibited a different trend. As shown in **Table 6**, the degree of change was essentially constant for no filler treatment, APS adsorption and allylamine grafting. These data are somewhat greater than the change observed for undecenylamine grafted E-glass bead filler. Similar to the Young's modulus data, the tensile strength of the pure epoxy did not decrease significantly upon hydrolytic exposure.

**Table 5. Young's Modulus of Composites After Hydrolytic Exposure**

	Young's Modulus (GPa)		
Filler Treatment	No Exposure	Hydrolytic Exposure	% Change
None	3.4	2.2	-35.3
Adsorbed APS	3.1	2.5	-19.4
Grafted Allylamine	3.7	2.3	-37.8
Grafted Undecenylamine	3.4	2.8	-17.6

Thus, when both data sets are considered simultaneously, the undecenylamine grafting treatment appears to give the best resistance to the type of hydrolytic exposure performed. The superiority of grafting with respect to no surface treatment and APS adsorption was expected due to the stability of the Si-C bond formed during grafting. The difference between the allyl- and undecenyl-amine grafting was unexpected, but may be due to the difference in chain length. The difference may be of particular importance on E-glass surfaces as full surface coverage is not necessarily expected, and thus, the longer chain of the undecenylamine graft may cover more of the surface, in the areas in which no grafting occurs, than the relatively short-chained allylamine graft. Therefore, more water is kept away from the surface by the undecenylamine graft and the hydrolytic stability of the surface is improved.

**Table 6. Tensile Strength of Composites After Hydrolytic Exposure**

Filler Treatment	Tensile Strength (MPa)		
	No Exposure	Hydrolytic Exposure	% Change
None	73.7	36.8	-50.1
Adsorbed APS	80.5	45.0	-44.1
Grafted Allylamine	62.5	34.0	-45.6
Grafted Undecenylamine	54.0	32.0	-31.5

## CONTINUOUS FIBER SURFACE MODIFICATION AND COMPOSITE FORMULATION AND TESTING

Next, the fabrication and testing of continuous fiber polymer matrix composite specimens was undertaken. The focus of these analyses was the effect of fiber ( $\text{SiO}_2$ ) treatment on composite performance under ambient and hygrothermal conditions. Several surface treatments were analyzed including direct grafting of silane coupling agents and traditional silane coupling agent adsorption. 3-point and 4-point bend testing were used for mechanical property analyses of the composite samples. It was found through 4-point bend testing that the flexural strength of the composite samples with directly grafted coupling agent retained a higher strength than the samples with the fibers having a traditional silane coupling agent treatment. Infrared analysis of both fibers and  $\text{SiO}_2$  single crystals showed indirect evidence of successful grafting of silane coupling agent. Because the Grignard reaction, in comparison with the Speier reaction, was an easier treatment method by which to modify E-glass beads, all surface modifications during this

reporting period were directed toward utilization of the Grignard reaction. More specifically, the Grignard reaction was used to modify (treat)  $\text{SiO}_2$  fiber surfaces with undecenyl groups. The treated fibers were characterized by FT-IR spectroscopy. Finally, the mechanical proprieties of surface treated (grafted and traditional silane coupling agent), continuous fibers reinforced polymer composites were tested to evaluate the hydrolytic stability.

### **Model System Selection**

Quartzel (Saint-Gobain) was chosen as the reinforcement fibers. Quartzel (+99.99%  $\text{SiO}_2$ ) fibers have a high modulus (78 GPa) and are continuous fibers and are supplied by the vendor with a layer of sizing on the surface. The Quartzel fibers have an average fiber diameter of 14  $\mu\text{m}$ . Derakane 470-300 (Dow Chemical Co.) an epoxy novolac-based vinyl ester was chosen as matrix material. Derakane was chosen as the matrix due to the likelihood of reaction between the vinyl groups of the matrix and the undecenyl groups on the  $\text{SiO}_2$  fiber surfaces.

### **Fiber Preparation**

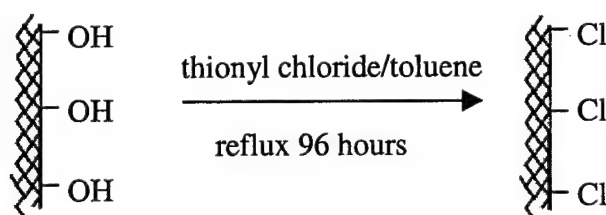
As mentioned above the as-received Quartzel fibers were coated with unknown sizing. Thus, to allow us to determine the effect of various surface treatments the fibers were cleaned with a room-temperature plasma asher to remove the sizing. Given the potential that the plasma treatment might cause dehydroxylation of the surface the fibers were rehydrated prior to any surface treatment. After the initial fiber preparations the fibers

were treated by the Grignard reaction to form the anticipated grafted coupling agents, or by adsorption of a traditional silane coupling agent.

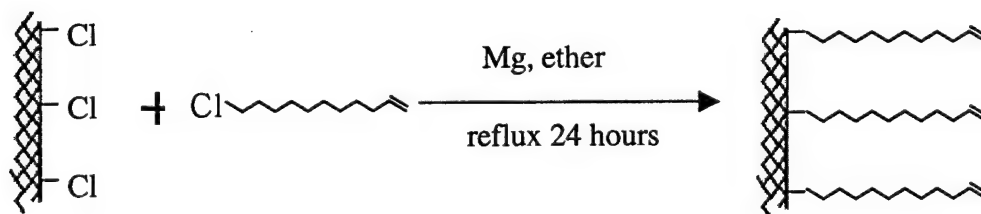
### Non-Traditional Silane Treatment

The treatment on the Quartzel fibers was accomplished by following the steps delineated below:

1. The fibers were chlorinated by refluxing in thionyl chloride/toluene solution for 96 hours.



2. The Grignard reaction was performed by reacting the chlorinated silica fibers with undecenylmagnesium halides, as shown below.



### Silane Treatment

The hydrated fibers were treated in aqueous solution with 0.5% (by weight)  $\gamma$ -aminopropyltrimethoxy silane (APS) to adsorb the coupling agent on the fiber surface. After adsorption the fibers were dried at 100°C for one hour, as is standard treatment procedure for traditional size coupling agents.

### **FT-IR Characterization**

Diffuse reflectance Fourier transform infrared spectroscopy (DRIFT) was used to characterize the treated Quartzel fibers. The DRIFT analysis required that the fibers be ground to fine powders using a standard mortar and pastel.

FT-IR spectra were taken before and after every step of treatments including the as-received, oxygen plasma-treated, hydrated, APS-treated, and Grignard-treated fibers for a comprehensive infrared analysis of the surface chemistry associated with each treatment. In addition, the hydrolytic stability of Grignard material on fiber surfaces was tested by exposing the surface-treated fibers to boiling, distilled water for one day. Fibers are then dried at room temperature, ground to fine powder and examined for FT-IR characterization. The amount of the grafted material remaining after 1 day boiling was determined by comparing the heights of the aliphatic CH<sub>2</sub> stretching bands at 2855 cm<sup>-1</sup> and 2925 cm<sup>-1</sup> before and after boiling.

**Figure 32** shows the comparison FT-IR spectra of as-received and plasma-treated fibers.

The disappearance of the bands aliphatic stretching bands at 2860 cm<sup>-1</sup>, 2920 cm<sup>-1</sup> and 2950 cm<sup>-1</sup> indicate the removal of the organic sizing from the as-received fibers. The spectra of plasma treated and hydrated fiber were non-descript, as the expected Si-H bands on the hydrated fibers were screened by the strong bands caused by water in the IR spectra.

**Figure 33** shows the spectra of plasma treated fibers with fibers after the Grignard treatments. Strong bands at  $2855\text{ cm}^{-1}$  and  $2925\text{ cm}^{-1}$  were observed after the Grignard reaction. The presence of these bands was an indication that an organic layer was grafted on the fiber surfaces. A band labeled  $\text{CH}_3$  in **Figure 33** around  $2950\text{ cm}^{-1}$  also appeared after grafting. The presence of this band was not expected. The appearance of  $\text{CH}_3$  band may be caused by the reaction of the vinyl groups grafted on the fiber surface. Further efforts are needed to determine the exact reason for this band's appearance.

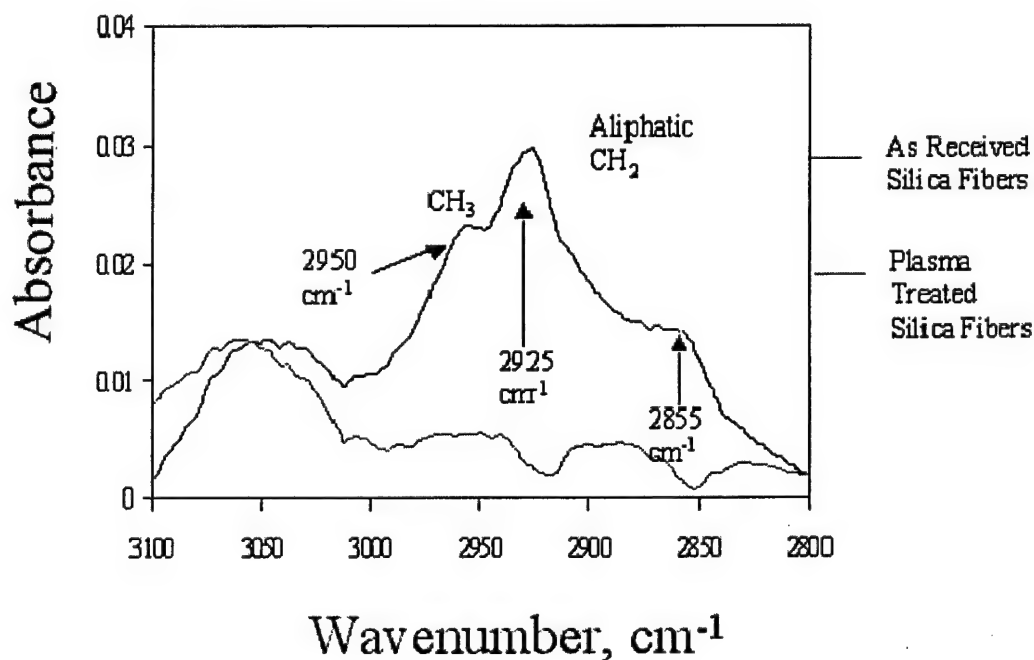


**Figure 32.** Comparison of as received silica fibers (top spectrum) with plasma treated fibers (bottom spectrum).

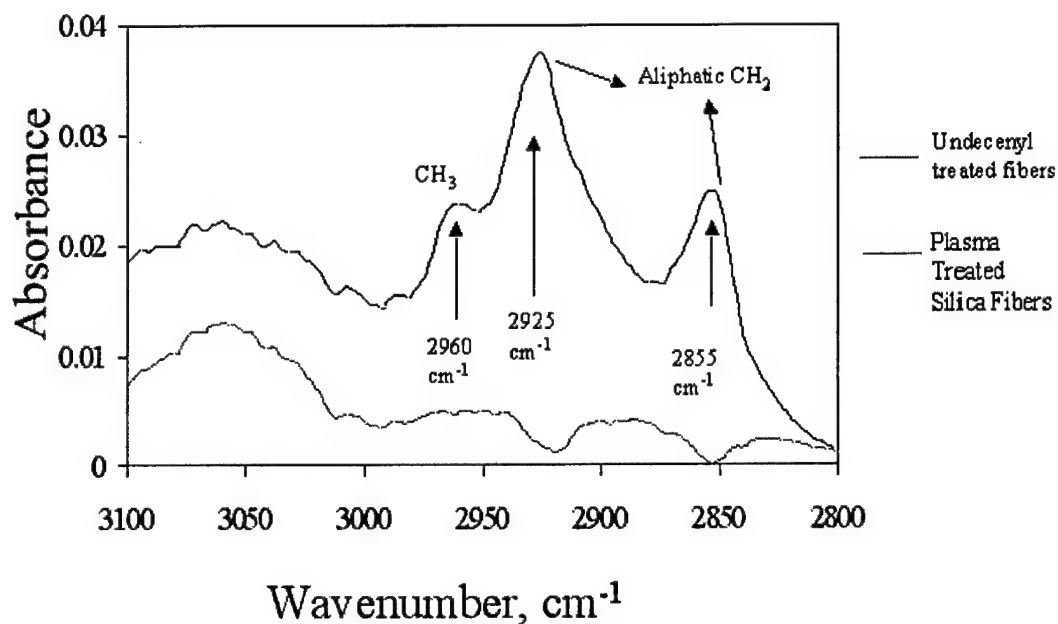


**Figure 33.** Comparison of undecenyl treated silica fibers (top spectrum) with plasma treated fibers (bottom spectrum).

**Figure 34** shows the spectra of plasma treated fibers with fibers after APS treatments.

Like in **Figure 33**, strong bands labeled  $\text{CH}_2$  at  $2855 \text{ cm}^{-1}$  and  $2925 \text{ cm}^{-1}$  were observed after APS treatment. These bands indicate desired APS on the fiber surfaces. Also, the  $\text{CH}_3$  band at around  $2960 \text{ cm}^{-1}$  was observed. The presence of this latter band was reasonable considering that not all the methyl groups in the APS may have hydrolyzed during the surface treatment.



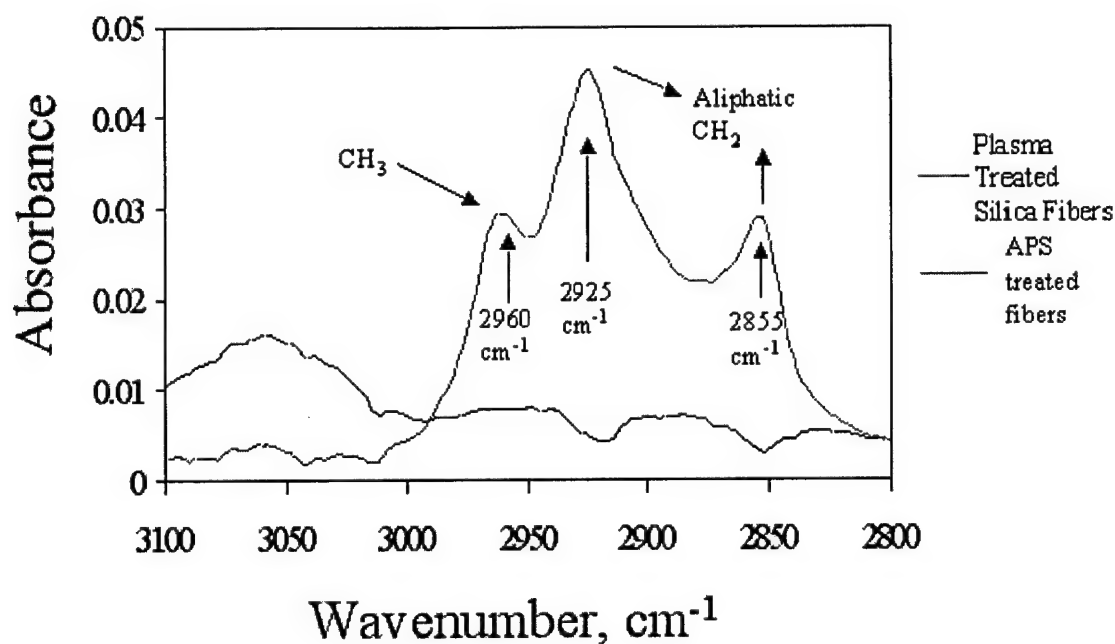


**Figure 34.** Comparison of APS treated silica fibers (top spectrum) with plasma treated fibers (bottom spectrum).

Fibers treated by the Grignard reaction were boiled for a day in water to evaluate the hydrolytic stability of the coupling agents. For comparison, APS treated fibers were also tested in this manner. **Figure 35** shows the spectra of fibers having directly Grignard coupling agents before and after boiling for 24 hours. As expected, all the bands in the initial spectrum have decreased by approximately the same amount. This indicates that some of the Grignard coupling agent was lost during boiling. **Figure 36** shows the spectra of APS treated fibers before and after boiling.

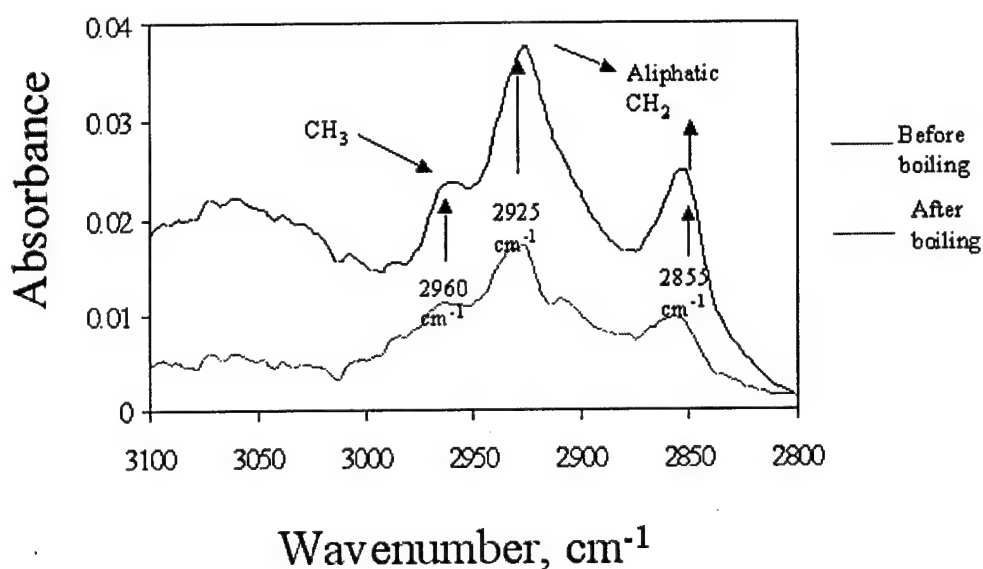


Figure 35. Comparison of undecenyl treated silica fibers before (top spectrum) and after boiling (bottom spectrum).

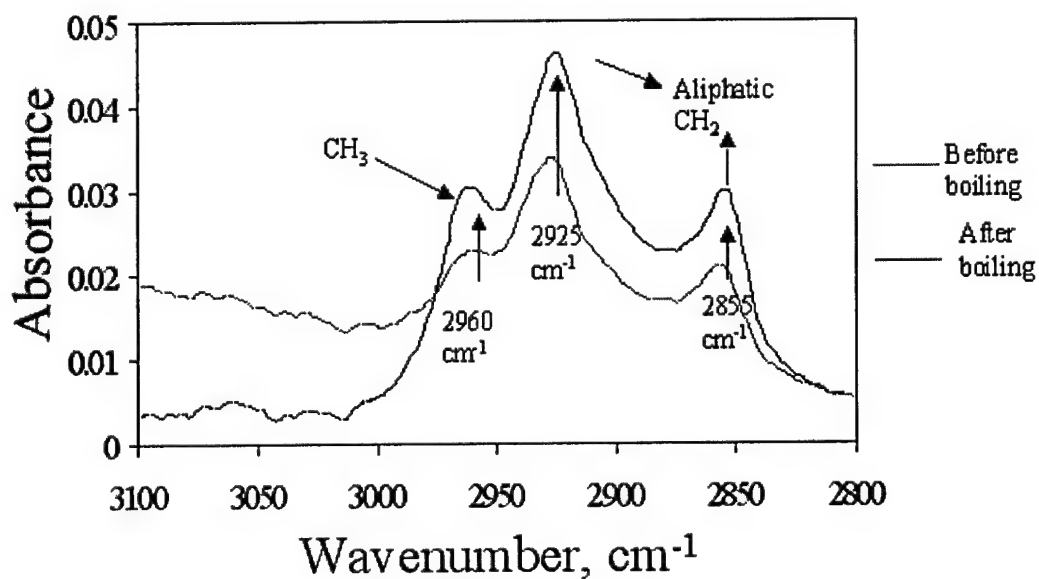


Figure 36. Comparison of APS treated silica fibers before (top spectrum) and after boiling (bottom spectrum).

Similar to **Figure 36**, band decrease was observed, indicating the loss of coupling agent.

**Table 7** shows the summary of the hydrolytic stability testing data. From the data in **Table 7** it appears that the Grignard material does not appear superior to APS in terms of the amount of material removed from the surface by boiling. About 50-55% of directly grafted undecenyl remained on the silica fiber surface after the boiling treatment. A similar amount remained of the APS.

**Table 7. Summary of FT-IR Hydrolytic Stability Data**

Surface Treatment	Percent remaining after 1 day boiling, %
Adsorbed APS	50-55
Grignard-Undecenyl	50-55

Next, polymer composites reinforced with surface treated Quartzel fibers were fabricated. The mechanical properties of the composites under different environmental conditions were tested and compared to evaluate the hydrolytic stability properties.

### **Mould Design and Fabrication**

A mould was designed to fabricate the continuous fiber composite samples. **Figures 37** and **38** show the schematic and photograph of the resulting mould.

### **Continuous Fiber Composite Specimen Fabrication**

A hand lay-up method was developed for placement of fibers within a sample. Optical microscopy was used to ensure that the fibers were placed uniformly and discretely within the sample. **Figure 39** shows a sample with the fibers placed prior to addition of the polymer matrix. Next, the resin (Derakane) was added to the system. Great care was

taken to avoid the formation of bubbles within the matrix. A room temperature polymer curing cycle was followed for initial samples.

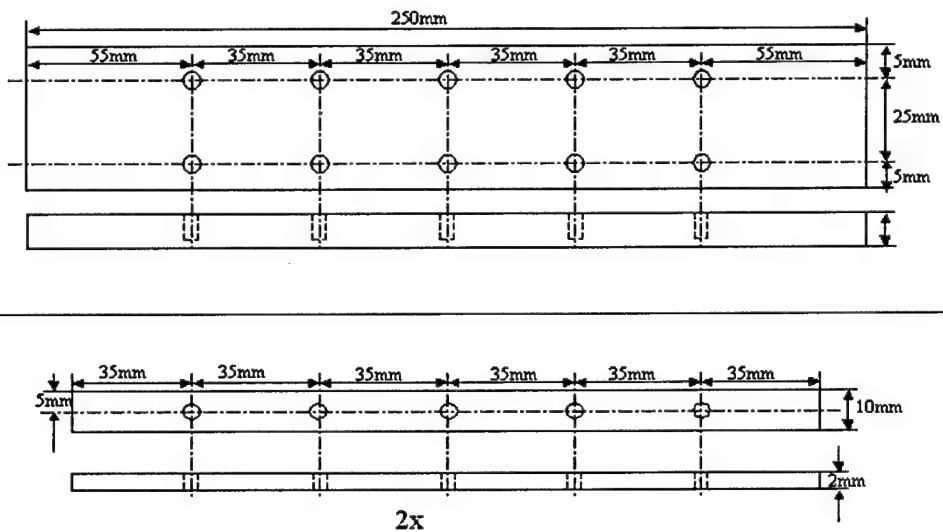


**Figure 37.** Schematic of mould for fabricating continuous fiber composite samples.

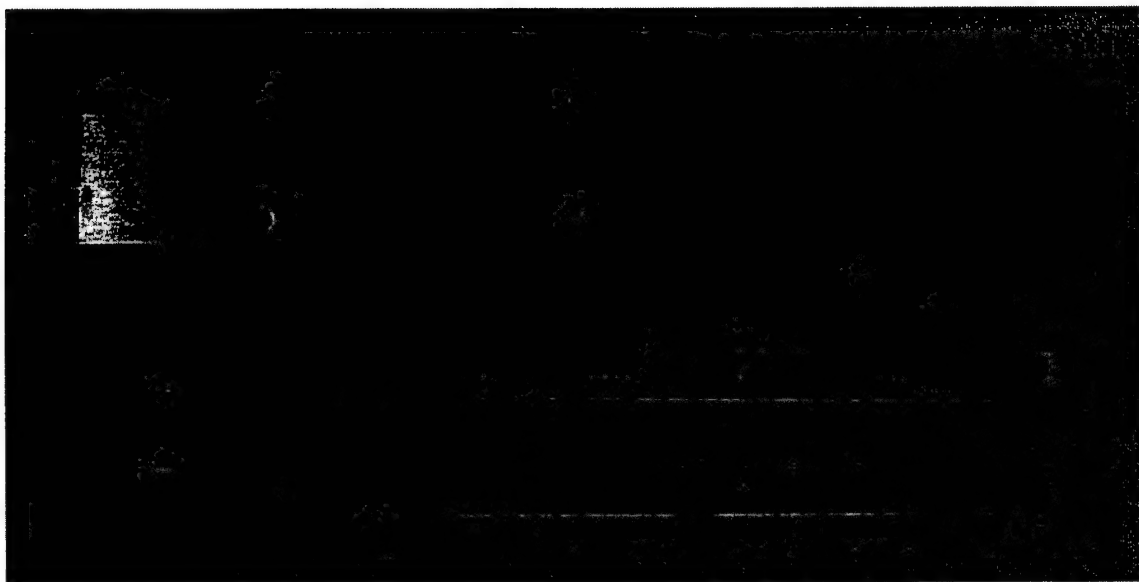


**Figure 38.** Picture of actual mould used for fabrication of continuous fiber composite samples.

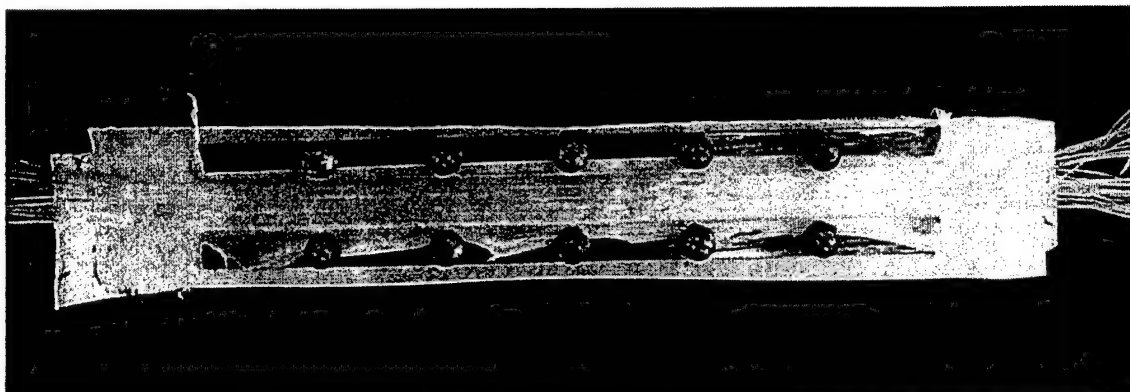


**Figure 39. Mould with fibers laid up.**

The mould allowed for fabrication of 5 samples for 3-point bend testing. Typical 3-point bend specimen are shown in **Figure 40**. Dimensions and other specification of the bend samples are listed in **Table 8**. **Figures 41 and 42** show pictures of a typical cross-sectional area of the samples. It can be concluded that homogenous dispersion of fibers within the polymer matrix was achieved.

**Table 8. Typical Dimensions and Specifications of Bend Test Samples**

<b>Length (mm)</b>	<b>Width (mm)</b>	<b>Height (mm)</b>	<b>Fiber content by volume (%)</b>	<b>Fiber content by weight (%)</b>
40	14	1.6	16.5	30

### **3-Point Bend Testing (Ambient Conditions)**

A miniature materials tester was used to perform the three point bending test of the composite samples. The test speed was 0.5 mm/min (ASTM standard D 790M) and the load was 1000 N. Five sample types were fabricated: pure resin, resin reinforced with

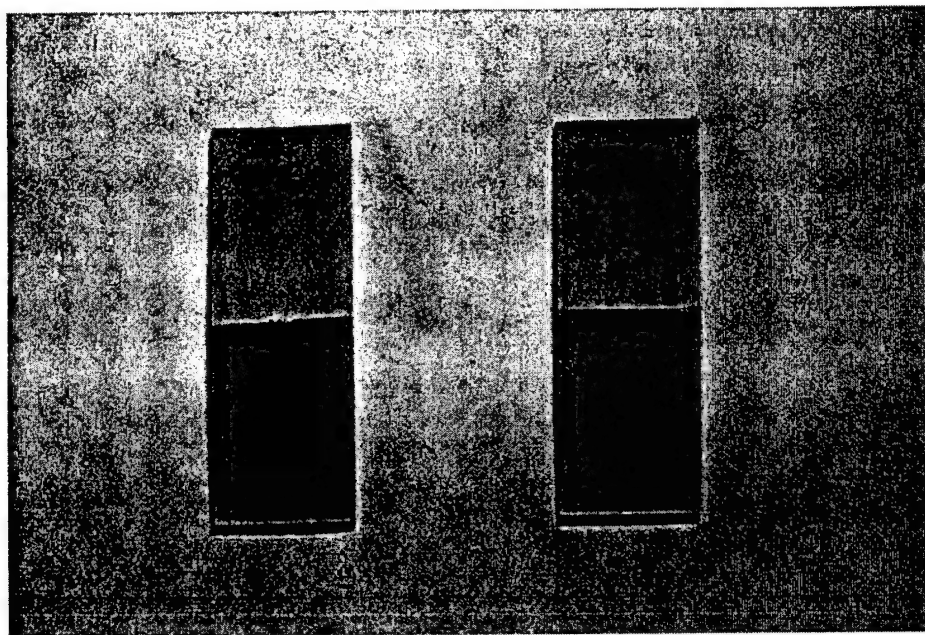


**Figure 40.** Picture of samples after 3-point bend testing.

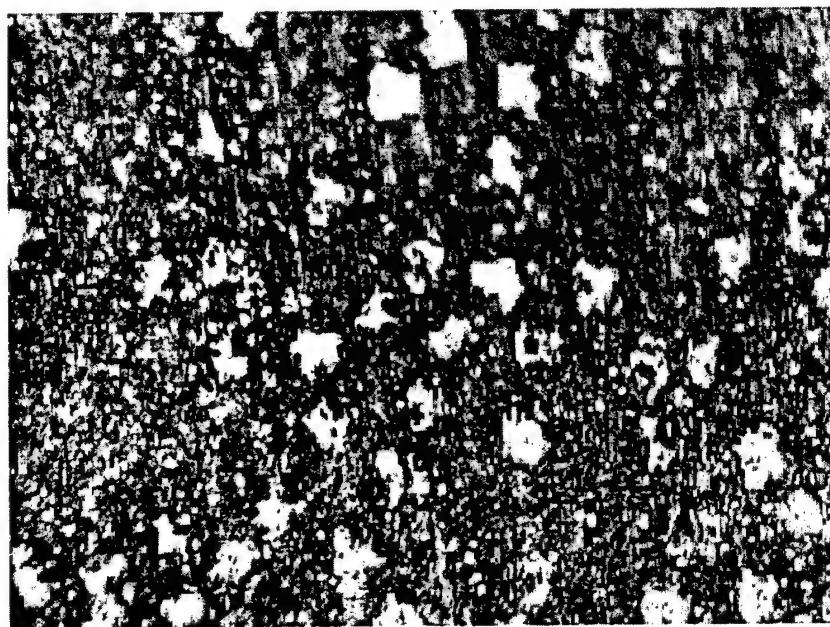


**Figure 41.** Optical image of  $\text{SiO}_2$  fibers within Derakane matrix (x50).

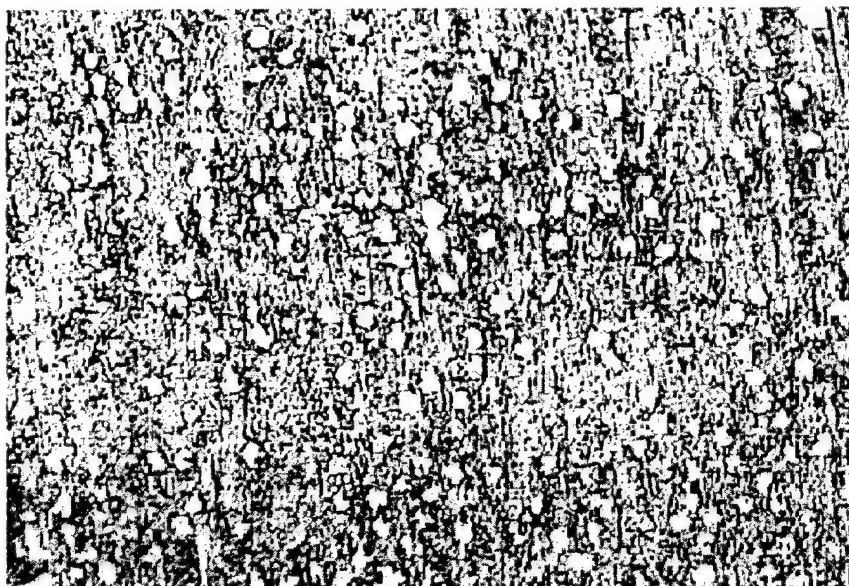


**Figure 42.** Optical image of SiO<sub>2</sub> fibers within Derakane matrix (x20).

plasma-cleaned fibers, resin reinforced with cleaned hydrated fibers, resin reinforced with APS treated fibers, and resin reinforced with undecenyl treated fibers. Five samples of each type were tested. The flexural strength and flexural modulus were measured and recorded for each sample. The standard deviations were calculated for each measurement category.

**Table 9** shows a summary of the 3-point bend testing results. It can be concluded that addition of fiber into Derakane, regardless of fiber surface treatment, increased the overall mechanical properties of the material. The flexural modulus increased by about a factor of 4 by fiber addition, as does the flexural strength. The results also indicated that different fiber surface treatments do not significantly change the flexural moduli of the composite samples. However, the various surface treatments did influence the flexural strength of the composites. The composites reinforced with APS treated fibers showed the highest flexural strength (390 MPa). Compared to samples reinforced with plasma-

treated and APS-treated fibers, composites reinforced with undecenyl-treated fibers show lower flexural strength (315 MPa). This can perhaps be explained by the fact that the handling required during the Grignard treatment is much more harsh than plasma and APS treatments, both in treatment time and frequency of handling. In other words, the treatment conditions will surely damage the mechanical properties of the fibers, and as consequence, the mechanical properties of the composites reinforced with the treated fibers will be thereby affected. The flexural strength of composites reinforced with Grignard treated fibers is much better than those reinforced with fibers after hydration (248 MPa), however, demonstrating that this method can improve the mechanical properties of the composites. Also, this result serves as an indirect indication that the undecenyl-treated fibers are coupling or co-reacting with the polymer matrix.

**Table 9. 3-Point Bend Testing Results (Ambient Conditions)**

<b>Fiber Surface Treatments</b>	<b>Flexural Modulus, GPa</b>	<b>Flexural Strength, MPa</b>
Matrix Only	$2.4 \pm 0.2$	$93.0 \pm 6.1$
Plasma Treatment Only	$9.2 \pm 0.5$	$365.0 \pm 14.5$
Hydration after Plasma	$9.2 \pm 0.2$	$248.0 \pm 41.7$
APS Treatment	$10.0 \pm 0.7$	$392.0 \pm 58.6$
Grignard/Undecenyl	$8.5 \pm 0.6$	$315.0 \pm 42.3$

### **3-Point Bend Testing (Hygrothermal Evaluation)**

Next, 5 samples of each type, as delineated earlier, were exposed to boiling distilled water for 24 and 48 hours, followed by three point bend testing. The results were



recorded and compared to those without boiling to study the hydrolytic stability of various surface treatments. **Tables 10-13** show the comparison of flexural moduli and flexural strengths of the composites sample before and after boiling for 24 and 48 hours. The flexural moduli of all samples increased after boiling. The increased flexural modulus was attributable to changes in the matrix as the pure matrix exhibited much higher flexural modulus after boiling. For example, after boiling for 48 hours, the flexural modulus of pure Derakane increased by about 62.5%. The flexural strengths, however, show a different trend. All composite samples, regardless of fiber surface treatment, exhibited a decrease in flexural strength after boiling for 24 hours and enhanced flexural strengths after boiling for 48 hours. One possible explanation for these results is that the resin was not fully cured at room temperature, prior to hygrothermal treatments. Therefore, the boiling water could decrease the strength of the samples by breaking the bonds in the interface between the polymer and fibers. On the other hand, the boiling water could also increase the strength by more fully curing of the polymer matrix. The competition between these two processes is evident in the first period 24 hours of boiling by the breaking of bonds in the fiber interface region while further boiling causes the influence of post-cure to become stronger, thus the strengths go up gradually after 48 hours of boiling. It was concluded that further work therefore needed to be done to optimize the curing process of the polymer matrix.

#### **Optimization of the Curing Schedule of Polymer**

Given the increase in strength noted above for the 48 hour boiling water treatment a series of tests were conducted to determine whether the polymer was fully cured by the

room temperature curing cycle recommended by the manufacturer. The objective of this series of tests was to be able to exclude the influence of temperature on the mechanical properties of polymer matrix, for subsequent composite tests. In this regard, 5 Derakane samples were each post cured at 100°C for 2 hours, 4 hours, 24 hours and 48 hours, respectively, after an initial room temperature cure for 24 hours. Three point bending tests were performed after each post cure. **Figures 43 and 44** show the flexural moduli and flexural strengths of Derakane samples with different post cure times. It can be concluded from the figures that elevated temperature can improve the mechanical properties of the polymer matrix in the first several hours, and further post cure after that will not cause much more improvement. **Table 14** shows the trend more clearly, both flexural strength and flexural modulus increased about 50% after post cure at 100°C for 4

**Table 10. Flexural Moduli of Composite Samples Before and After Exposure to Boiling Water for 24 Hours**

Fiber Treatment	Flexural Modulus (GPa)		
	No Exposure	Hydrolytic Exposure	% Change
None	2.4 ± 0.2	N/A	N/A
Plasma	9.2 ± 0.5	10.8 ± 0.2	17.4
Hydration	9.2 ± 0.2	9.9 ± 0.8	7.6
Absorbed APS	10.0 ± 0.7	10.4 ± 0.7	4.0
Grignard/Undecenyl	8.5 ± 0.6	11.2 ± 2.1	31.8

**Table 11. Flexural Moduli of Composite Samples Before and After Exposure to Boiling Water for 48 Hours**

	Flexural Modulus (GPa)		
Fiber Treatment	No Exposure	Hydrolytic Exposure	% Change
None	2.4 ± 0.2	3.9 ± 0.2	62.5
Plasma	9.2 ± 0.5	11.2 ± 0.2	21.7
Hydration	9.2 ± 0.2	10.8 ± 0.2	17.4
Absorbed APS	10.0 ± 0.7	10.8 ± 0.7	8.0
Grignard/Undecenyl	8.5 ± 0.6	10.0 ± 0.4	17.6

**Table 12. Flexural Strength of Composite Samples Before and After Exposure to Boiling Water for 24 Hours**

	Flexural Strength, MPa		
Fiber Treatment	No Exposure	Hydrolytic Exposure	% Change
None	93.0 ± 6.1	N/A	N/A
Plasma	365.0 ± 14.5	332.0 ± 13.6	-9.0
Hydration	248.0 ± 41.7	270.0 ± 18.1	-7.8
Absorbed APS	392.0 ± 58.6	378.0 ± 44.0	-0.5
Grignard/Undecenyl	315.0 ± 42.3	309.0 ± 14.0	-2.8

**Table 13. Flexural Strength of Composite Samples Before and After Exposure to Boiling Water for 48 Hours**

<b>Fiber Treatment</b>	<b>Flexural Strength, MPa</b>		
	<b>No Exposure</b>	<b>Hydrolytic Exposure</b>	<b>% Change</b>
None	93.0 ± 6.1	138.0 ± 19.3	48.4
Plasma	365.0 ± 14.5	385.0 ± 30.9	5.5
Hydration	248.0 ± 41.7	366.0 ± 28.5	24.9
Adsorbed APS	392.0 ± 58.6	426.0 ± 76.3	12.1
Grignard/Undecenyl	315.0 ± 42.3	380.0 ± 36.7	19.5

hours. After 4 hours, no improvements were observed. Therefore a 5 hours post cure at 100°C, after the room temperature cure for 24 hours, was adopted as an optimized curing process for Derakane and was used in all subsequent testing.

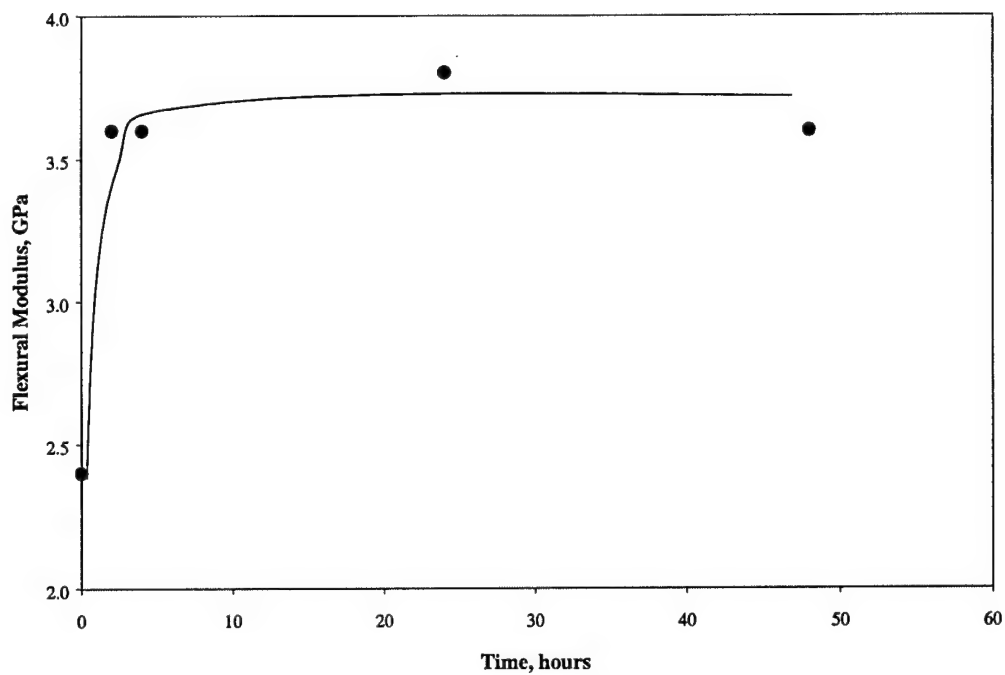


**Figure 43.** Change of flexural moduli of Derakane with time at elevated temperature (post cure at 100°C).

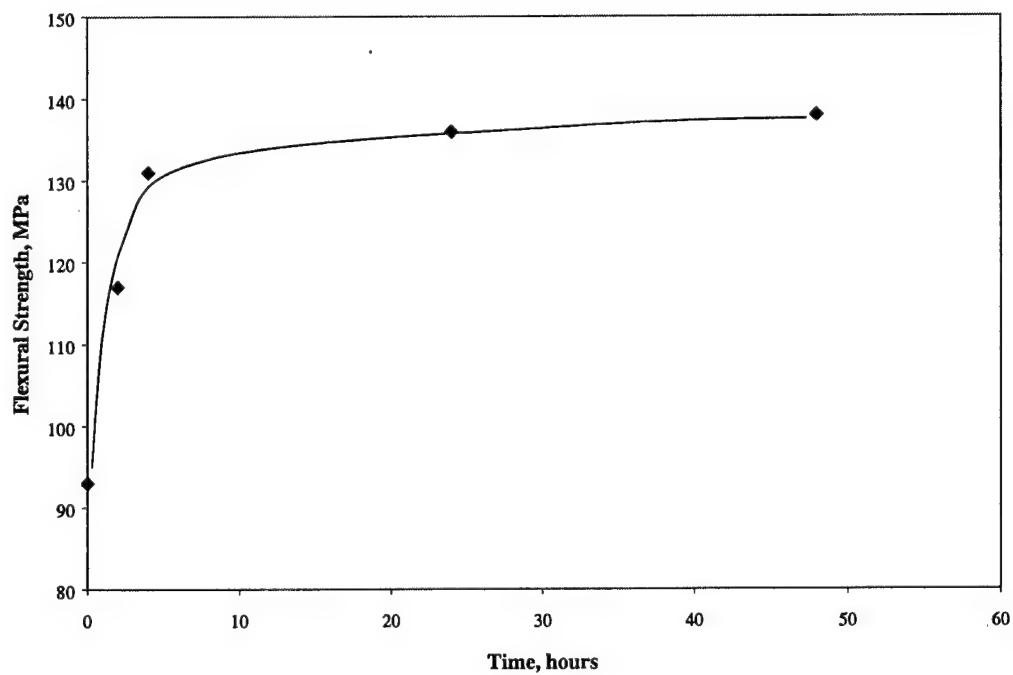


**Figure 44.** Change of flexural strength of Derakane with time at elevated temperature (post cure at 100°C).

**Table 14. Mechanical Property Data of Derakane with Time at Elevated Temperature (Post Cure at 100°C)**

Time, hours	Flexural Strength, MPa	Flexural Modulus, GPa
0	93	2.4
2	117	3.6
4	131	3.6
24	136	3.8
48	138	3.6

#### **4-Point Bend Testing (Hygrothermal Evaluation)**

Like the 3-point bending test, the 4-point bending test is a standard test method to study the flexural properties of unreinforced polymer composites. The advantage of the 4-point bending test is that the influences of the fiber/matrix interfaces are more pronounced.

After discussion of the relative merits of each test with colleagues at the annual AFOSR Performance Review in Long Beach, CA (May, 2002) it was decided that for this work, which hinges upon fiber surface treatment, that the 4-point test was the better of the two tests. Because the grip for the four point bending test was not commercially available, a new grip specified by ATSM D 790M was designed and machined. **Figure 45** shows the comparisons of broken samples after 3-point bending test and 4-point bending test. The sample after 4-point bending test has a larger broken region, hence the interfaces between

the organic polymer and inorganic fibers plays a more important role than in the 3-point test.

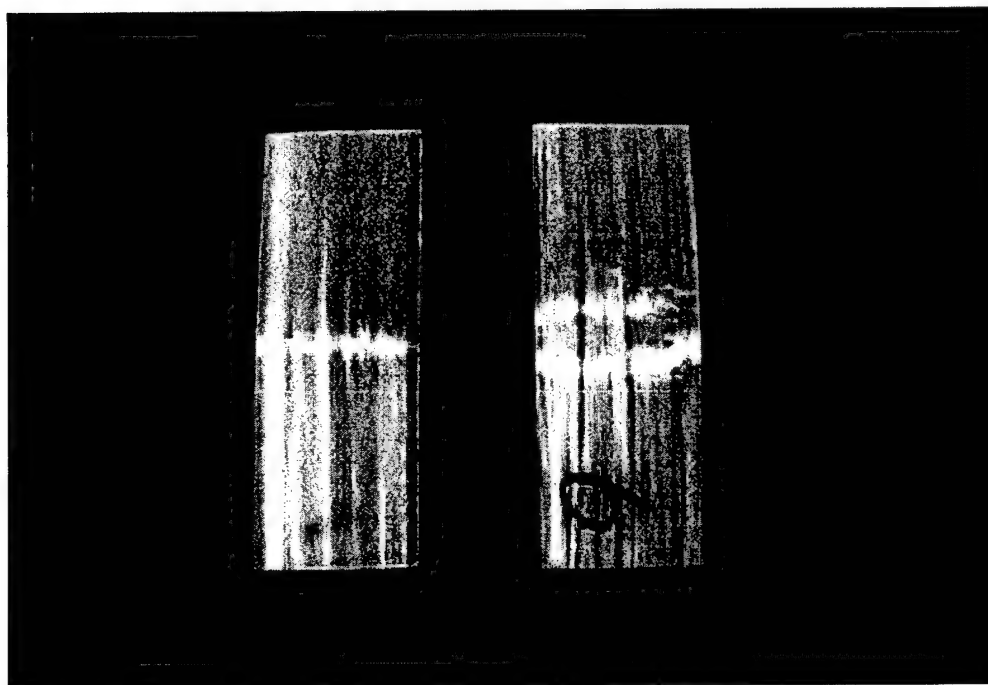


**Figure 45.** Comparison of broken samples after 3-point bending test and 4-point bending.

The testing parameters for 4-point bending tests were the same as specified earlier for 3-point testing, with the exception of the new grip mentioned earlier. Also, the 5 sample types were the same as specified earlier, with the only difference in the composite fabrication being the optimized cure cycle of Derakane. Five samples of each type were exposed to boiling distilled water for 48 hours followed by 4-point bending tests. Test results were recorded and compared with those without boiling to study the hydrolytic stability of various surface treatments.

**Table 15** is the summary of the four point bending test results under ambient conditions. Similar to the 3-point results, the different fiber surface treatments did not significantly change the flexural modulus of the composite samples. Similar to the results in 3-point bending tests, composites reinforced with plasma treated fiber have the highest flexural strengths (523 MPa). The reason for the high flexural strength of the plasma treated fibers is believed to be do the very high surface energy of the bare SiO<sub>2</sub> fibers which promotes wetting by polar organics like Derakane, and also possibly those fibers have been through the least physical handling compared to the other fiber treatment types studied. Compared to reinforced hydrated fibers, composites reinforced with APS treated and directly grafted fibers show higher strengths. This is expected, as by definition, coupling agents should enhance the adhesion between fiber and matrix, and hence, the strength of the composite. Importantly, composites reinforced with fibers having directly grafted coupling agents have higher strength compared to those reinforced with APS treated fibers, indicating that the directly grafted coupling agents have better coupling ability.

**Table 15. 4-Point Bend Testing Results (Ambient Conditions)**

<b>Fiber Surface Treatment</b>	<b>Flexural Modulus, GPa</b>	<b>Flexural Strength, MPa</b>
Matrix Only	4.5 ± 0.4	144 ± 18.5
Plasma Only	13.1 ± 1.6	523 ± 24.4
Hydration after Plasma	12.4 ± 1.0	340 ± 44.7
APS Treatment	11.0 ± 1.9	391 ± 37.8
Grignard/Undecenyl	13.2 ± 0.6	473 ± 39.5



Next, composite sample were boiled for 48 hours in distilled water followed by 4-point bending testing. **Table 16** shows the comparison of flexural moduli before and after boiling. The values before and after boiling cannot really be differentiated. **Table 17** lists a comparison of flexural strengths before and after boiling. Pure Derakane and

**Table 16. Flexural Moduli of Composite Samples Before and After Exposure to Boiling Water for 48 Hours**

Fiber Treatment	Flexural Modulus, GPa		
	No Exposure	Hydrolytic Exposure	% Change
Matrix Only	4.5 ± 0.4	4.1 ± 0.1	-8.9%
Plasma	13.1 ± 1.6	12.8 ± 0.3	-2.3%
Hydration	12.4 ± 1.0	13.0 ± 0.5	4.8%
Absorbed APS	11.0 ± 1.9	11.7 ± 0.7	6.4%
Grignard/Undecenyl	13.2 ± 0.6	12.8 ± 1.0	-3.0%

**Table 17. Flexural Strength of Composite Samples Before and After Exposure to Boiling Water for 48 Hours**

Fiber Treatment	Flexural Strength, MPa		
	No Exposure	Hydrolytic Exposure	% Change
Matrix Only	144 ± 18.5	82.0 ± 9.9	-28.1%
Plasma	523 ± 24.4	375.0 ± 30.1	-28.3%
Hydration	340 ± 44.7	317.0 ± 22.7	-6.8%
Adsorbed APS	391 ± 37.8	389.0 ± 29.7	-0.5%
Grignard/Undecenyl	473 ± 39.5	429.0 ± 42.7	-9.3%

composites reinforced with plasma-treated fibers show deteriorated strength, dropping by about 28%. This drop in strength is most likely due to the freshly formed silica surface being hydrolytically very unstable. The strengths of composites reinforced with other fibers do not show as much decrease in strength after boiling. *Composites reinforced with Grignard treated fibers were found to be superior to those reinforced with APS treated fibers when the absolute values of strengths are compared.*

## **WEATHERING OF SURFACE-MODIFIED, SINGLE FIBERS AND CONTINUOUS-FIBER COMPOSITE MATERIALS**

The final area investigated was weathering of single fibers to determine the ability of the various surface treatments to ameliorate weathering effects. In addition, a long-term weathering cycle, similar to a typical airplane's daily weather exposure, was utilized for testing continuous-fiber reinforced composite materials.

### **Single Fiber Weathering Tests**

Single fiber tensile testing was performed to further investigate the effects of hydrolytic exposure on the modified fibers used in this work. This testing was performed according to the ASTM 3379-75 standard test. In the test procedure, individual fibers were fixed to two metal plates separated by 80 mm on a plate holding device. The plateholder was designed to force the fiber to be placed along the centerline. The metal plates with attached fiber were then placed into the grips of the Minimat miniature materials tester. The fiber was then pulled until broken. The force at breakage was recorded. For each treatment, several fibers, typically eight, were tested. The data generated by this testing

was fit to a two-parameter Weibull distribution (Equation 2). The various treatments were compared by examining the characteristic strength; the  $\sigma_0$  parameter.

$$F = 1 - \exp((-\sigma/\sigma_0)^m) \quad (2)$$

where  $F = (I-0.3)/(J+0.4)$  is the failure probability using the median rank method in which  $I$  is the rank of each observation and  $J$  is the total number of observations in a given data set. The value  $\sigma$  is the strength of the individual fiber, while  $\sigma_0$  and  $m$  are the two Weibull parameters. **Table 18** shows the characteristic fiber strength data and the range for this parameter for the different fiber surface treatments utilized. For instance, for plasma treated fibers that were not subjected to weathering, the characteristic fiber strength is 216.7 MPa with the 95% confidence interval of this parameter being 202.1 to 255.7 MPa. From the data in **Table 18**, the characteristic strength of the fibers decreased with more handling in the absence of weathering. The plasma treated fibers characteristic strength was 216.7 MPa, hydrating decreased this strength to 207.9 MPa, adsorbing aminopropyltrimethoxy silane (APS) to the surface decreased the strength to 184.3 MPa and grafting undecenyl bromide to the fiber's surface reduce the characteristic strength to 167.4 MPa. This trend is expected in that hydration followed plasma treatment and the APS and grafting treatments followed the hydration step; more handling is involved in each treatment step and increased handling leads to more surface flaws and hence lower strength.. As described previously, the APS treatment involved less handling and stirring than the grafted treatment. The confidence interval data show that the differences between the plasma treatment and hydration treatment are minimal; and, that the APS and grafted treatments are not statistically different in terms of fiber strength.

Comparison of the unweathered fiber strengths to the fiber strengths after boiling in water for 24 hours data is also found in **Table 18**. This data shows that the plasma treated (-45%), hydrated (-35%) and APS treated (-20%) fiber strengths decreased considerably, at least 20%, while the grafted fiber strengths did not decrease at all. This once again shows the ability of the Si-C bonds made through grafting to resist water attack. Therefore, this data shows that the grafted fibers were more hydrolytically stable than untreated fibers and even APS treated fibers.

**Table 18. Characteristic Fiber Strength (Mean) and 95% Confidence Interval (95% CI) for Various Fiber Treatments**

	Plasma		Hydrated		APS		Grafted	
	Mean	95% CI	Mean	95% CI	Mean	95% CI	Mean	95% CI
Unweathered	216.7	255.7	207.9	237.2	184.3	192.7	167.4	198.0
		-		-		-		-
		202.1		197.9		179.9		160.7
24-Hour Boil	141.1	176.2	115.2	133.2	146.8	174.9	187.8	280.0
		-		-		-		-
		130.2		108.9		138.0		164.8

### Long Term Weathering Tests

Previously, all samples were subjected to short-term weathering, in which the samples were put into boiling water for 24 and 48 hours. In practical use, composite samples will have a more long-term exposure in adverse environmental conditions that are less severe than boiling water. Therefore, continuous fiber composite samples were exposed to environmental conditions similar to those airplanes might experience.

An environmental cycle was developed based on the possible conditions, including temperature and atmosphere, experienced by aircraft. The environmental cycle utilized is shown in the **Figure 46**.

The specimens were exposed to the environmental cycle 5 days a week; the other two days they were stored at 50°C and 95-100% relative humidity. To perform the environmental cycle, specimens were placed into a sealed container. This container was then placed into an oven set to the desired temperature. The relative humidity was maintained by putting an aqueous salt solution in the container. The salt solution used to maintain relative humidity was selected according to the ASTM standards E-104. **Table 19** indicates the relationship between relative humidity and the temperature.

To treat a group of samples according to the long-term weathering test (see **Figure 46**), a beaker with the potassium sulfate saturated aqueous salt solutions was placed into a container, and samples were suspended within the container. In this manner the samples were kept at relative humidity around 96% at 50°C (see **Table 19**). For the 25°C test portion, the relative humidity is provided by saturated  $\text{Mg}(\text{NO}_3)_2 \cdot 6\text{H}_2\text{O}$  aqueous solution, as shown in **Table 19**.

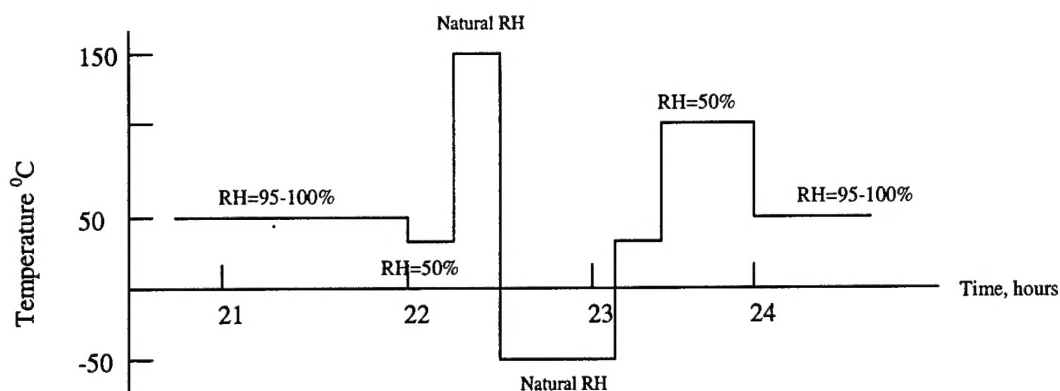


**Figure 46.** Environmental cycle, representative of the temperature /humidity condition an aircraft may meet during actual use. RH stands for relative humidity.

**Table 19.** The Relative Humidity and Salt Solution Abridged from ASTM E-104

T, °C	Mg(NO <sub>3</sub> ) <sub>2</sub> ·6H <sub>2</sub> O	K <sub>2</sub> SO <sub>4</sub>
0	60.4±0.6	98.8±2.1
5	58.9±0.4	98.5±0.9
10	57.4±0.3	98.2±0.8
15	55.9±0.3	97.9±0.6
20	54.4±0.2	97.6±0.5
25	52.9±0.2	97.3±0.5
30	51.4±0.2	97.0±0.4
35	49.9±0.3	96.7±0.4
40	48.4±0.4	96.4±0.4
45	46.9±0.5	96.1±0.4
50	45.4±0.6	95.8±0.5

After five weeks following the weathering cycle in **Figure 46**, the weathered samples were subjected to four-point bending tests. The four-point bending test set-up was designed previously for this project according to ATSM D 790M. The flexural modulus and flexural strength of the samples were calculated from the resulting data at a test speed of 0.5 mm/min.

The samples tested included the Derakane matrix with no reinforcement (no fibers), and four reinforced samples. The reinforcements were plasma treated fibers (plasma only), plasma treated that had been rehydrated (hydration after plasma), rehydrated fibers to which APS had been adsorbed (APS treatment) and rehydrated fibers subjected to the Grignard process grafting.

**Table 20. Average Flexural Modulus and Strength Before and After Long-Term Weathering**

Fiber Surface Treatment	Average Flexural Modulus (MPa)			Average Flexural Strength (MPa)		
	Before weathering	After weathering	Change	Before weathering	After weathering	Change
No Fibers	4.2 ±1.0	3.5±0.8	-16.7%	114.0±14.8	84.0±16.4	-26.3%
Plasma Only	10.6±1.2	9.6±1.0	-9.4%	362.0±73.3	292.0±44.0	-19.3%
Hydration after Plasma	13.4±2.3	10.9±2.4	-18.7%	379.0±49.0	344.0±106	-9.2%
APS Treatment	10.8±2.2	12.6±1.7	16.7%	290.0±55.1	425.0±119	46.6%
Direct Grafting	13.1±1.5	11.5±1.3	-12.2%	320.0±63.7	294.0±55.1	-8.1%

The results shown in **Table 20** are somewhat inconclusive. However, all treatments except the APS treatment showed about the same decrease in flexural modulus. In terms of flexural strength, the pure matrix and plasma treated fiber reinforced samples showed significant decreases in strength of approximately 20-25%, while the hydrated and grafted samples showed a much smaller decrease of slightly less than 10%. Similar to the flexural modulus, the Derakane reinforced with APS treated fibers showed an increase in flexural strength. The most likely cause of the APS treated sample's behavior was that the interfacial region between the fiber and the matrix, and in particular, APS and the

matrix are continuing to react over the 5 weeks of the long-term weathering test. This could cause an increase in the strength and modulus for the composite piece, which would negate the decrease in properties due to weathering effects.

For the more pertinent issue of the grafted material's behavior, the long-term weathering behavior is very similar to that of the short-term 48-hour boiling. For all the groups of samples tested except the APS, the modulus decrease was slightly greater in the long-term weathering case, while the strength decrease was slightly less with long-term weathering. Thus, the short-term experiments provide a good measure of the long-term behavior. Therefore, grafting of undecenylbromide to quartz surfaces provided excellent hydrolytic stability for the resulting composite material.

### **RECOMMENDATIONS FOR FUTURE RESEARCH**

The research conducted herein was performed on a variety of substrates including microspheres, optical planes, and reinforcing fibers. Grafting successfully modified all substrates studied. In order to further maximize the knowledge-base created by the research it is recommended that continuing research be pursued.

First, the majority of the research concerning the identification and quantification of the grafted layers was indirect and utilized techniques including contact angle and FT-IR spectroscopy to determine the presence/absence of covalently-modified surfaces. A more direct and detailed direct analysis is now warranted. Toward this end, comprehensive x-ray photoelectron spectroscopic (XPS) analysis should be performed. Preliminary XPS



analysis has been done in conjunction with the Environmental Molecular Sciences Laboratory at Pacific Northwest National Laboratory, and a detailed XPS study would serve to demonstrate more comprehensively the results of the indirect analyses reported here.

Second, efforts should be devoted to optimize the grafting reactions with the objective of maximizing surface coverage. Contact angle measurements indicated that ~80% of surface coverage was due to grafting. It is not clear, however, if the approximate 20% of surface not covered was because of lack of available hydroxyl species on the surface to be grafted or due to unfavorable conditions in the grafting methodology employed.

Third, effort may productively be directed toward the investigation of structure-property relationships of different grafting coupling agents in terms of (1) polarity, and (2) chain length. This recommendation is given because of the statistically limited trials of employed chain polarities and lengths examined in this research. A further examination is warranted to both optimize the materials employed in this research in terms of methodology, as well as to explore potentially more efficacious molecular coupling agents as suggested in this study.